Radar basis

Mehrez ZRIBI

CESBIO

ACTIVE/PASSIVE REMOTE SENSING

Passive observation
The source is the sun
•Radiometer
•Camera

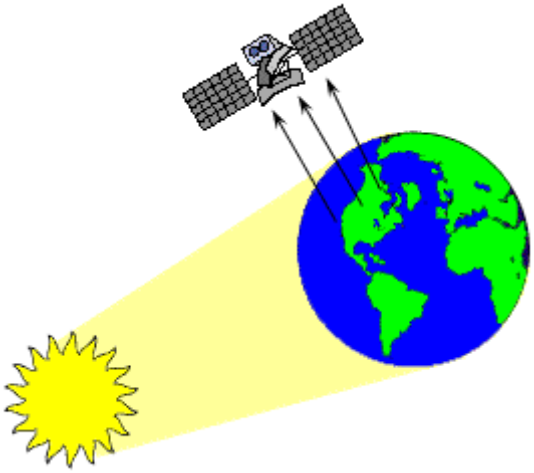

Active observation
The source comes from the instrument
•LIDAR
•RADAR

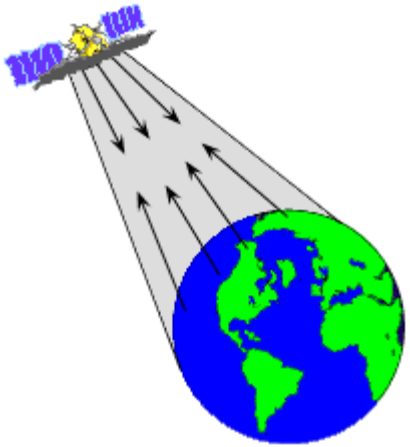

THE FREQUENCY RANGE OF MICROWAVES

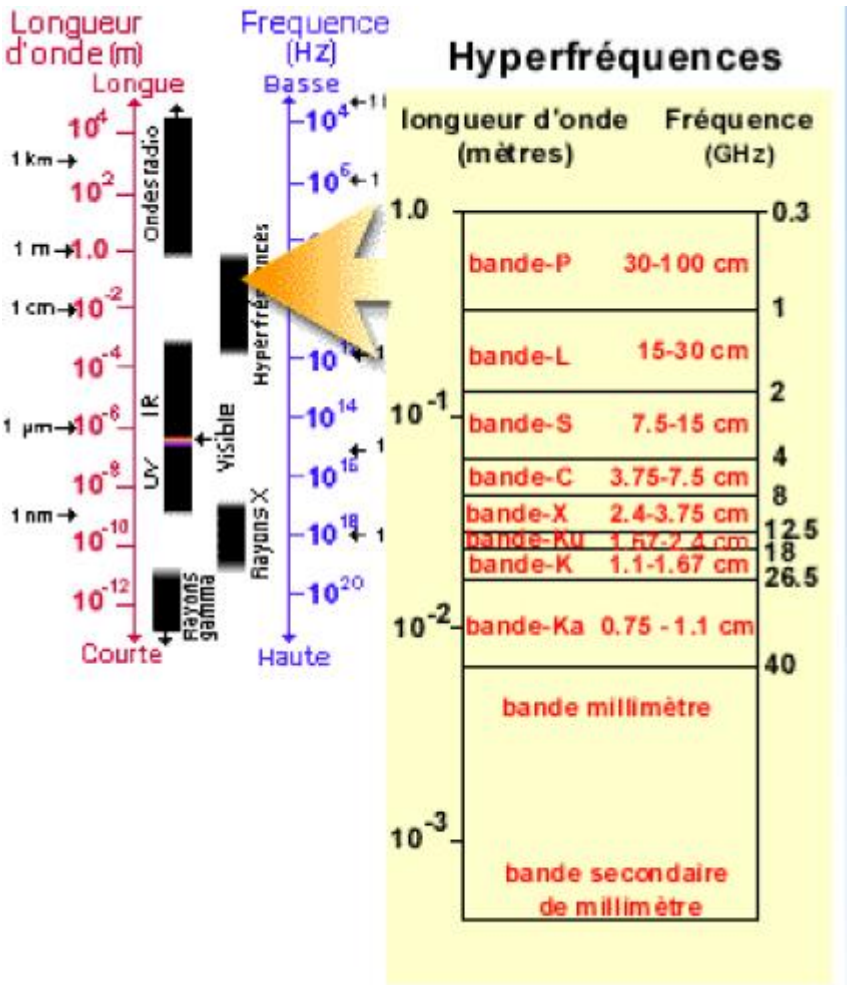

RADAR

FROM P BAND TO KA BAND

$$\lambda = \frac{C}{f}$$

$$k = \frac{2\pi}{\lambda}$$

Radar basis

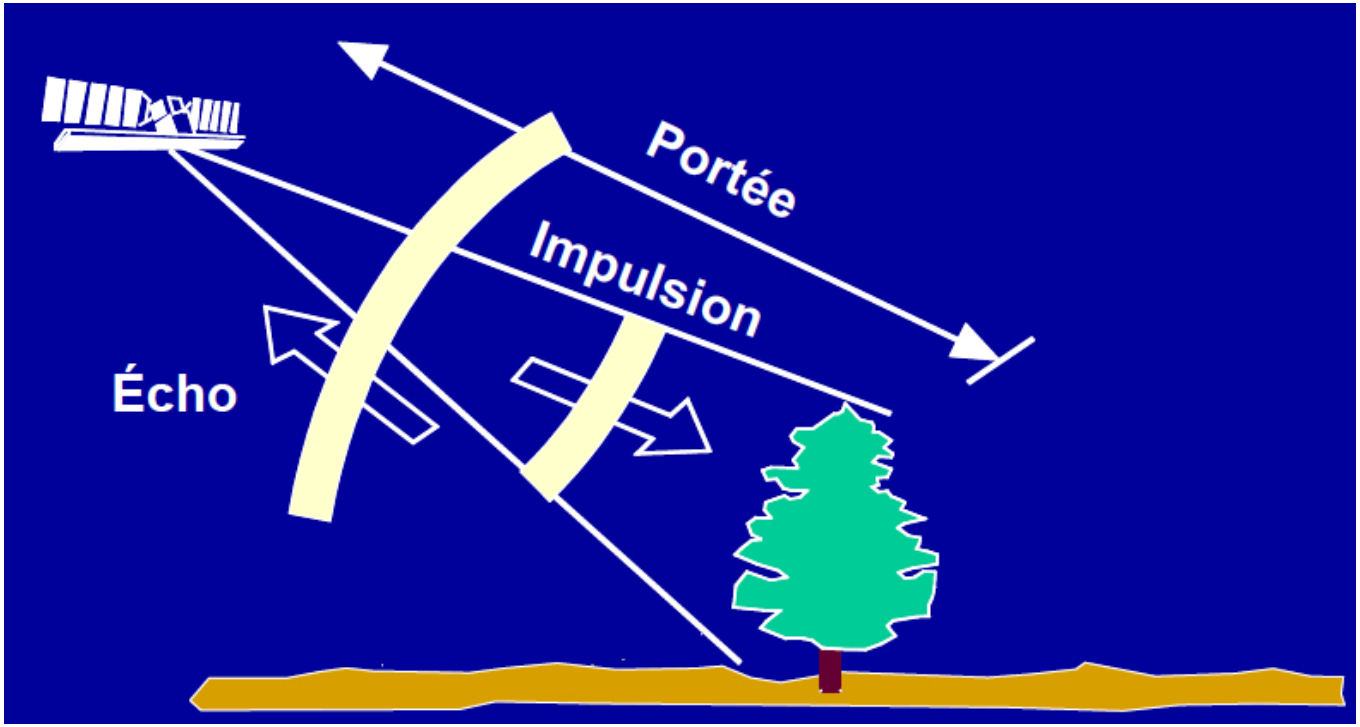

The radar itself provides the required energy:
→ It can therefore be used at both day and night

Microwaves in the field of radar are not very sensitive to the atmosphere:
→ The radar works even under cloud cover

1) RADAR EQUATION

The radar equation reflects the influence of physical phenomena on the radiated power, the wave propagation, and until the reflected signal (echo) is received. The radar equation provides an estimate of the performance of a radar system.

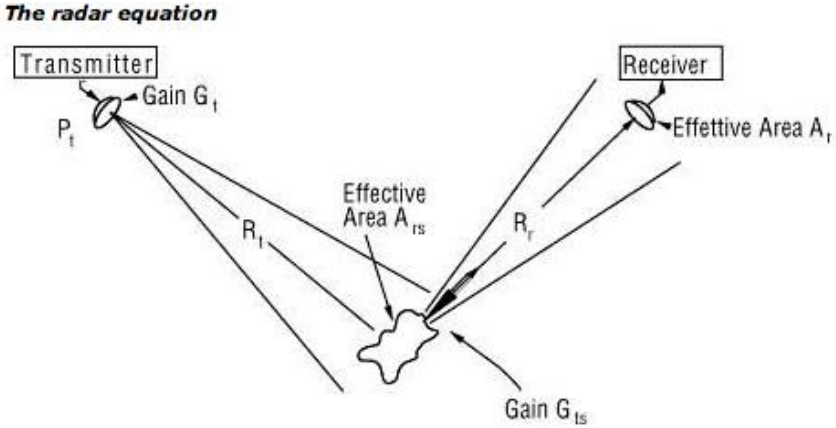

Considering *Pe* : power emitted by radar ;
R : distance target-radar ;

$$Ss = \frac{PeGe}{4\pi R^2}$$ The incident flux at the target surface

$$\frac{1}{4\pi R^2}$$ The loss factor linked to propagation of wave in the vacuum

Pis = Ss Ars is the power intercepted by the scatterer: equal to power density multiplied by the effective area of the scatterer

1) RADAR EQUATION

The effective area is a quantity dependent on the target and indicates its power of greater or lesser reflection. It depends on the form, the nature and its materials Constituents as well as the one of the wavelength, of the incidence.
A part of the power received is absorbed, the other part is returned directions.

Absorbed fraction *fa* Reflected fraction *1-fa*

Reflected power Pts=Pis (1-fa)

The scatterer behaves like an antenna, the power density that returns to the receiver is:

$$S_t = P_{ts} G_{ts} \left(\frac{1}{4\pi R_t^2} \right)$$

The power at receiver is : $P_r = S_t A_{rt}$

$$P_r = P_t G_t \left(\frac{1}{4\pi R_t^2} \right) A_{rs} (1 - f_a) G_{ts} \left(\frac{1}{4\pi R^2} \right) A_{rt}$$

1) RADAR EQUATION

- **The radar cross-section** or the backscattering effective surface area is combined in a single factor if the transmitter and receiver are in the same location (radar case). This factor depends on the incident and reflected wave of the shape and the dielectric properties of the diffuser

$$\sigma = A_{rs}\left(1 - f_a\right)G_{ts}$$

- The radar equation is written:

$$P_r = \frac{P_t G_t A_{rt}}{(4\pi)^2 R^4}\sigma$$

$$G_t = G_r = G$$

$$A_t = A_r = A$$

$$P_r = \frac{P_t G^2 \lambda^2}{(4\pi)^3 R^4}\sigma$$

Ae the effective surface of antenna, is linked to gain by:

$$Ae = \frac{G_R \lambda^2}{4\pi}$$

The radar coefficient or radar backscatter coefficient is defined as σ_0

In the case of punctual target $\sigma_0 = \sigma$

In the case of extended target $\sigma_0 = \frac{\sigma}{A}$

1) RADAR EQUATION

In the case of an extended target
The signal is an amplitude and phase combination of the elementary signals
From each surface element, shifted by **2R/c** at emission

$$P_r = \frac{P_t G^2 \lambda^2}{(4\pi)^3 R^4} \sigma_0 A \qquad \langle \mathrm{Pr} \rangle = \frac{\lambda^2}{(4\pi)^3} P_e \iint_s G_t G_r \frac{1}{R^4} \sigma^0(r) dS$$

The integral is performed on the observed surface *S*, delimited by the main lobe of the antenna. Assuming that the target is sufficiently far from the radar and therefore that all points are at equal distance *R* = *R0* and that σ0 is constant on the observed surface, the equation reduces to:

$$\langle \mathrm{Pr} \rangle = \frac{\lambda^2}{(4\pi)^3} P_e \frac{1}{R_0^4} \sigma^0(R0) \iint_s G_t(r) G_r(r) dS$$

For the observation of the surfaces, one calculates σ0 from the received power and by applying the radar equation. From σ0, we deduce, for a configuration of the given system (frequency, Incidence, polarization), surface characteristics of the target using models that link σ0 to the characteristics of the surface.

1) RADAR EQUATION

Since the radar backscatter coefficient σ0 has a high dynamic range, it is often chosen to express it in decibels:

$$\sigma_{dB}^{0} = 10 \log \sigma^{0}(\theta)$$

The radar backscatter coefficient is also defined as the ratio of the total power isotropically scattered by a diffuser equivalent to the incident power density occurring on the target. Its expression is:

$$\sigma = 4\pi \lim_{r \to \infty} r^{2} \frac{|E_s|^2}{|E_i|^2}$$

2) Principal technical and technological choices for satellite sensors

a) Frequency choice

- The carrier frequency is one of the essential technical characteristics.
- This is the result of a number of constraints, mainly:

→Regulatory constraints,

→Thematic objectives,

→Technological and technical constraints,

→Overall mission / platform constraints.

Regulatory constraints

These are constraints due to the regulations of the International Telecommunication Union (ITU), limitations linked to other missions (terrestrial primary services, etc.).

Thematic objectives

The observed media, which are essentially large and natural targets, can be roughly classified into three categories: Rainfall (precipitation rates to be measured) The sea (wind, surface) Vegetation and soils (roughness, humidity, vegetation, ...)

Technological and technical constraints

It is to study the feasibility or not (at a reasonable cost of course) of elements of the radar (amplifier, antenna, signal generator, ...). Example of constraints: the size of the antenna (to be put under the cap of the satellite launcher).

Mission constraints

This is a more general level (system including the ground segment, for example: effects of atmospheric disturbance, etc.).

b) Polarisation

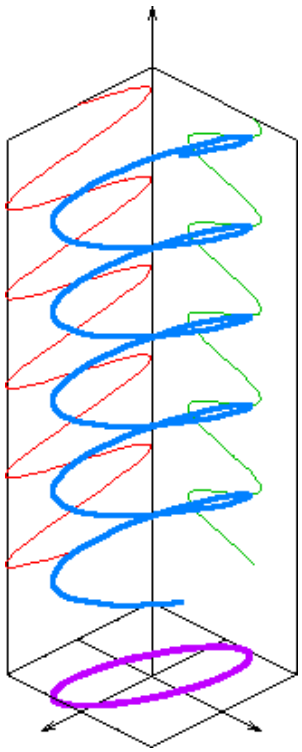

- At a great distance from the radiation sources (antennas) and in the main radiation lobe, the electromagnetic field is constituted by transverse vibrations perpendicular to the direction of propagation. **Both electric field and magnetic field are perpendicular**. The two vibrate at the same frequency and with proportional amplitudes.
- **The direction of polarization of the wave is that of the electric field E**. In the general case, the vector E rotates one complete revolution during an alternation. It is then shown that its end describes an ellipse, it is said that the polarization is elliptic.

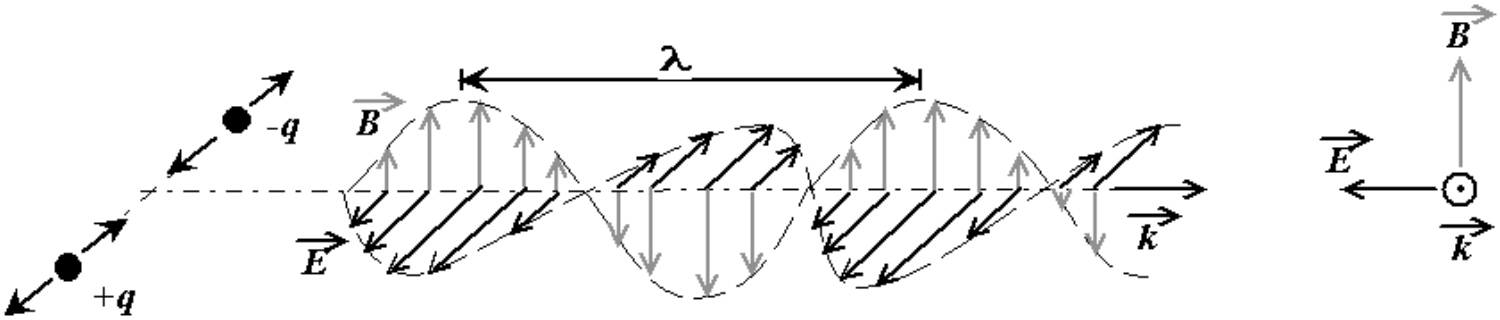

- Particular cases :
- **Circular polarization** (equal axes of the ellipse)
- **Linear polarization** (vector E maintains a fixed direction, completely flattened ellipse).

In the spatial case, only linear polarization is used (simpler). The polarizations are called **V** if the vector E is contained in the plane of incidence and **H** if the vector E is perpendicular to this plane It will be possible to receive in the same polarization as at emission, which corresponds to the configurations named for example **HH** and **VV** (or possibly crossed **HV**). The signals are strong when the elements are oriented in the same direction as the polarization of the incident wave.

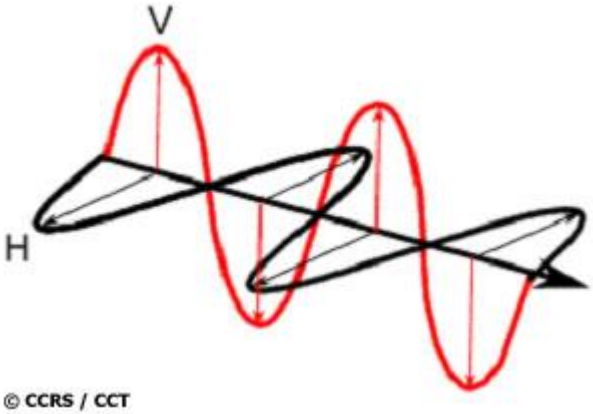

Polarimetric radar

A polarimetric radar allows the measurement of all the terms of the scattering matrix:

$$E_s = \begin{bmatrix} S11 & S12 \\ S21 & S22 \end{bmatrix} E_i$$

HH HV VV Composed image

c) spatial resolution of radar

- The spatial resolution of the radar translates the notion of separating power and decorrelation of the measurements made.
- It is the result of the geometrical resolution related to the antenna and a temporal resolution related to the pulses:

  - first, on the ground, the main lobe of the antenna defines an area on which the radar is measuring. Then the radar transmits pulses, modulated or not, depending on the radioelectric axis of the antenna or the distance axis. After reception and adapted processing of these pulses, a response of the radar defining its range resolution is obtained along the range axis, thus forming remote gates.

d) Radiometric resolution

- It characterizes the residual fluctuation of the measurement of the backscattered power after spatial or temporal average of N cells of mean power PR in the presence of a noise power B.
- The radiometric accuracy of the measurement can be defined either absolutely or relative. Absolutely, it expresses the total bias of the backscatter coefficient over the duration of the radar mission. It includes all the causes of error and inaccuracy on the measure, among others:
- uncertainty on antenna gain Ge GR, - antenna deployment effects - inaccuracy of the internal radar calibration - effects of atmospheric attenuation - effects of possible non-linearities in reception.
- An accuracy of less than 1 dB in absolute radiometric resolution is sought for most space radars (altimeter, SAR, scatterometer).
- Then a relative notion can be defined. For example, for observations at different instants in SAR, a relative accuracy better than 1 dB may be sought.

3) Absoluate calibration
a) punctual targets

- Objective: identification of the absolute value of the radar measurement
- Insufficiently accurate calibration will result in poor scattering interpretation
- Use of point targets whose radar signature is known (trihedrons, dihedrons, ...)
- At lower frequencies, larger reflectors are used since the power of the returned signal is proportional to the square of the radar frequency

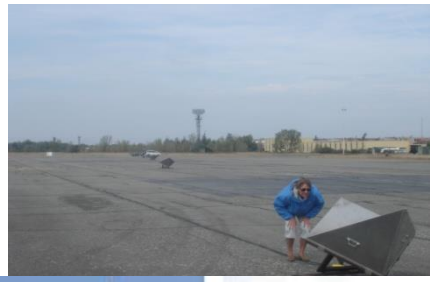

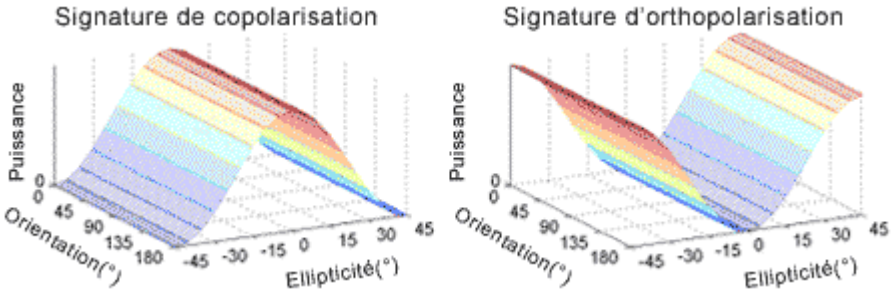

Polarimetric signature of a trihedron reflector.

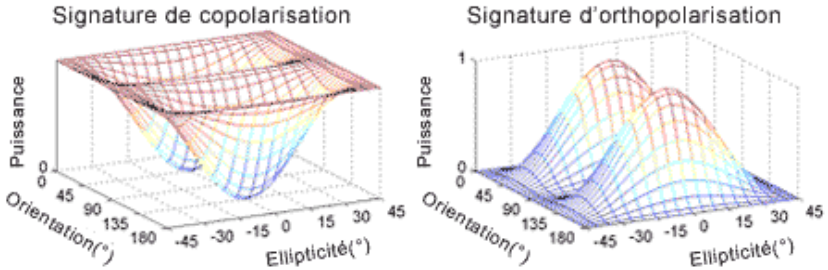

Polarimetric signatures of a dihedron

b) extended targets

- Using extended targets whose signature does not change with time
- Exemple: amazonien forest, deserts, antarc ...tic

4) Principal types of spatial radars

- Altimeter
- SAR
- scatterometer

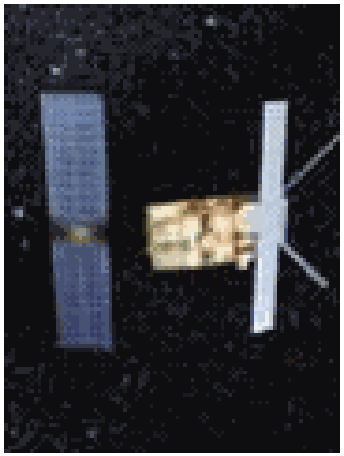

Altimeters

Space altimetry is a technique for measuring satellite heights. It uses the time taken by a radar beam to make the satellite-to-surface round-trip, associated with a precise location of the satellite, to carry out its measurements. An altimeter radar on board a satellite transmits a very high frequency signal (more than 1700 pulses per second) vertically to the ground and receives in return the echo reflected by the surface of the sea The analysis of the echo makes it possible to extract a very precise measurement of the travel time between the satellite and the sea surface, as well as the height of the waves and the speed of the wind. This time is then transformed into a distance by simple multiplication by the speed of light, the rate at which the emitted electromagnetic waves propagate.
Exemples: TOPEX/POSEIDON, JASON

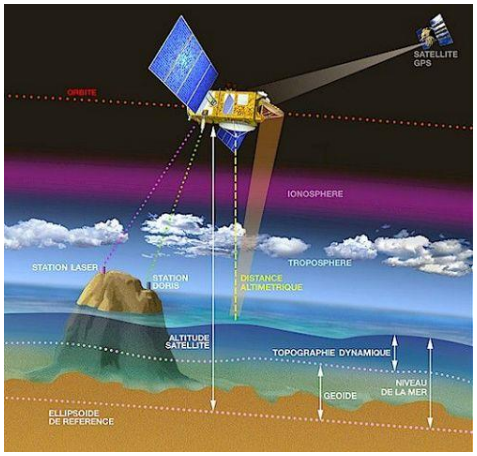

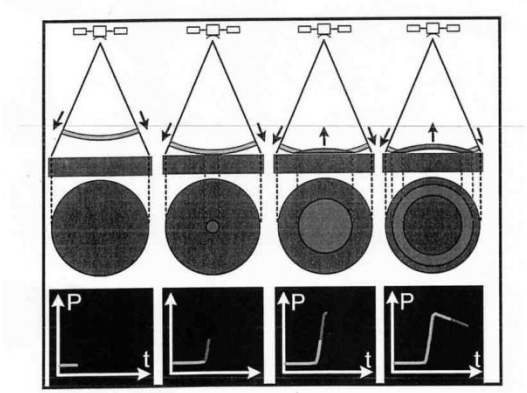

Applications

- Sea level
- Hydrology
- Geodesy
- Glaciology

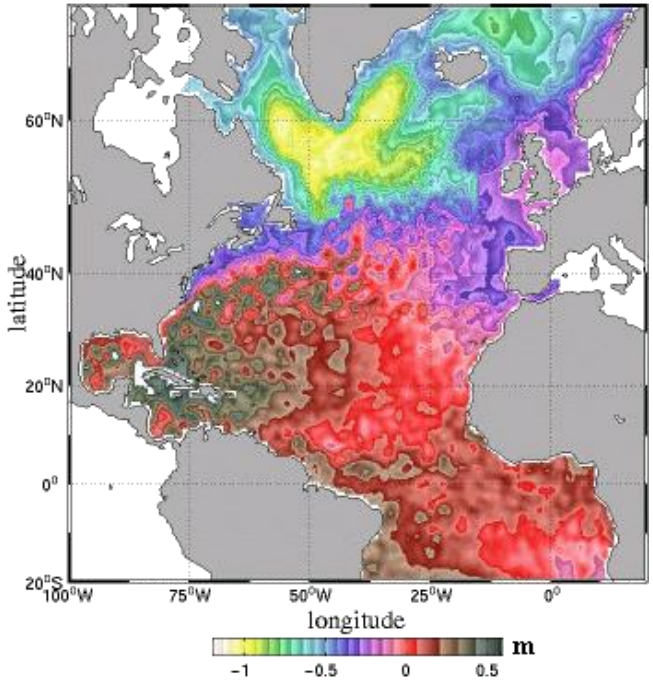

Water level

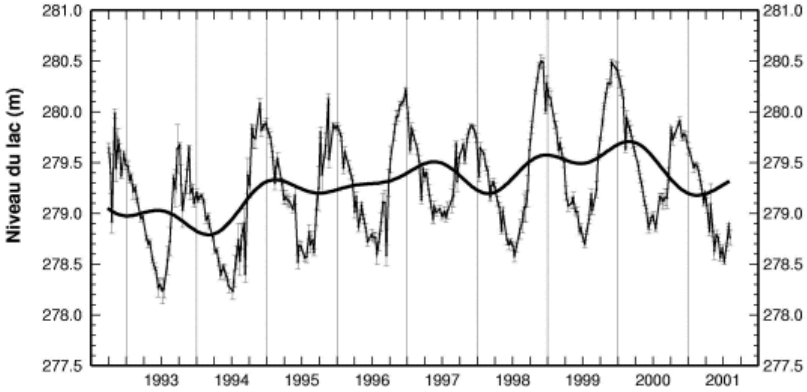

Level of Tchad lac

Scatterometers

Radar, low spatial resolution, multi-configurations

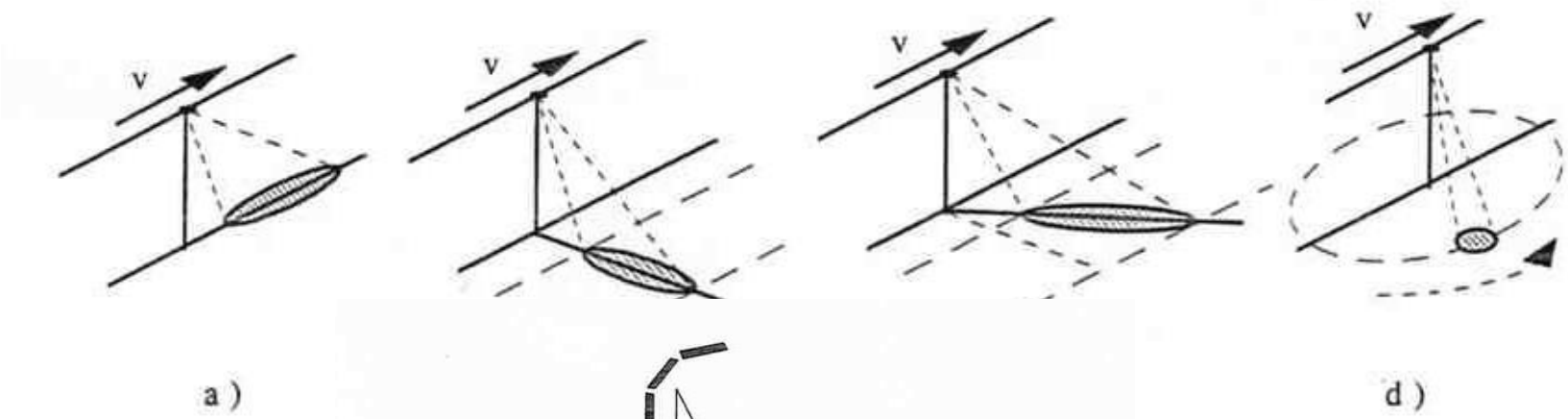

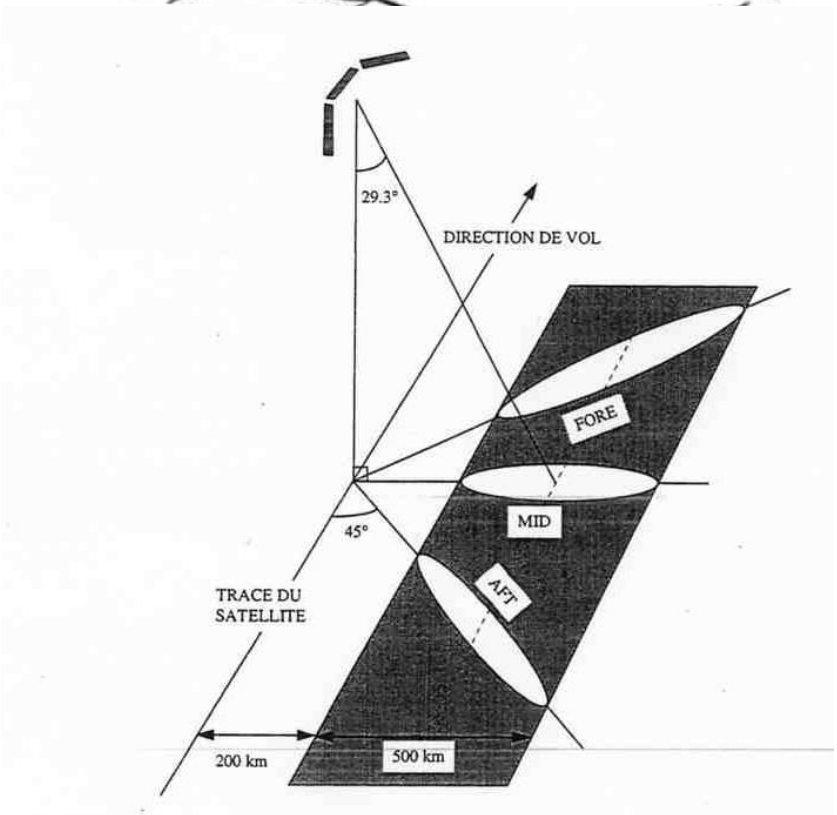

Applications

- Wind direction
- Ice mapping
- Continental surfaces (inondations, moisture, vegetation, ..)

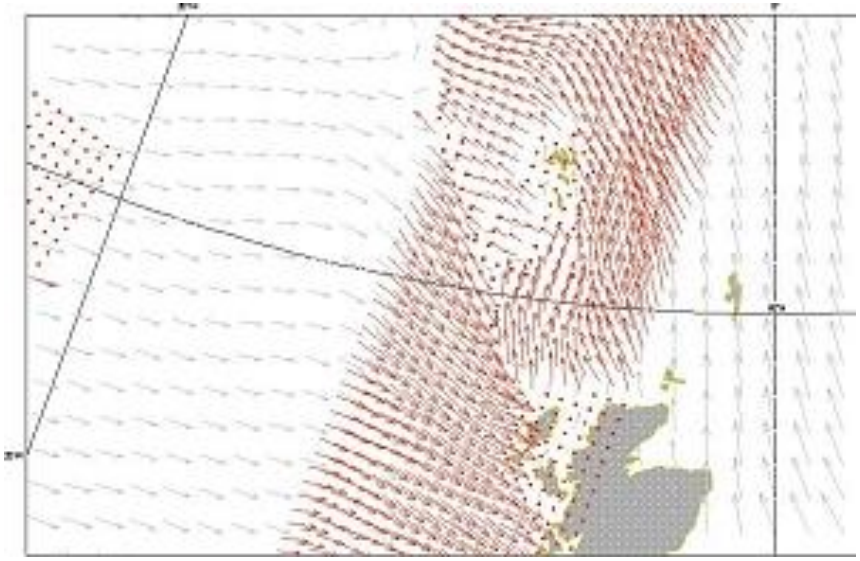

Wind direction

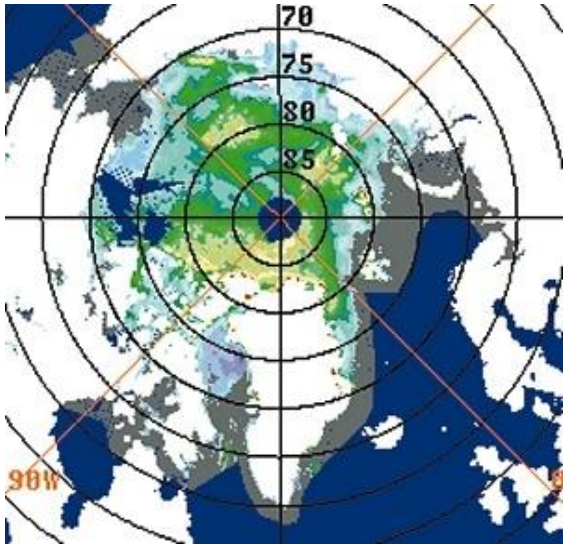

Ice mapping

Exemple: ERS, ASCAT/METOP, Quickscat

5) Synthetic Aperture Radar (SAR)

Radar image, ERS2, VV, C band, chott Jerid

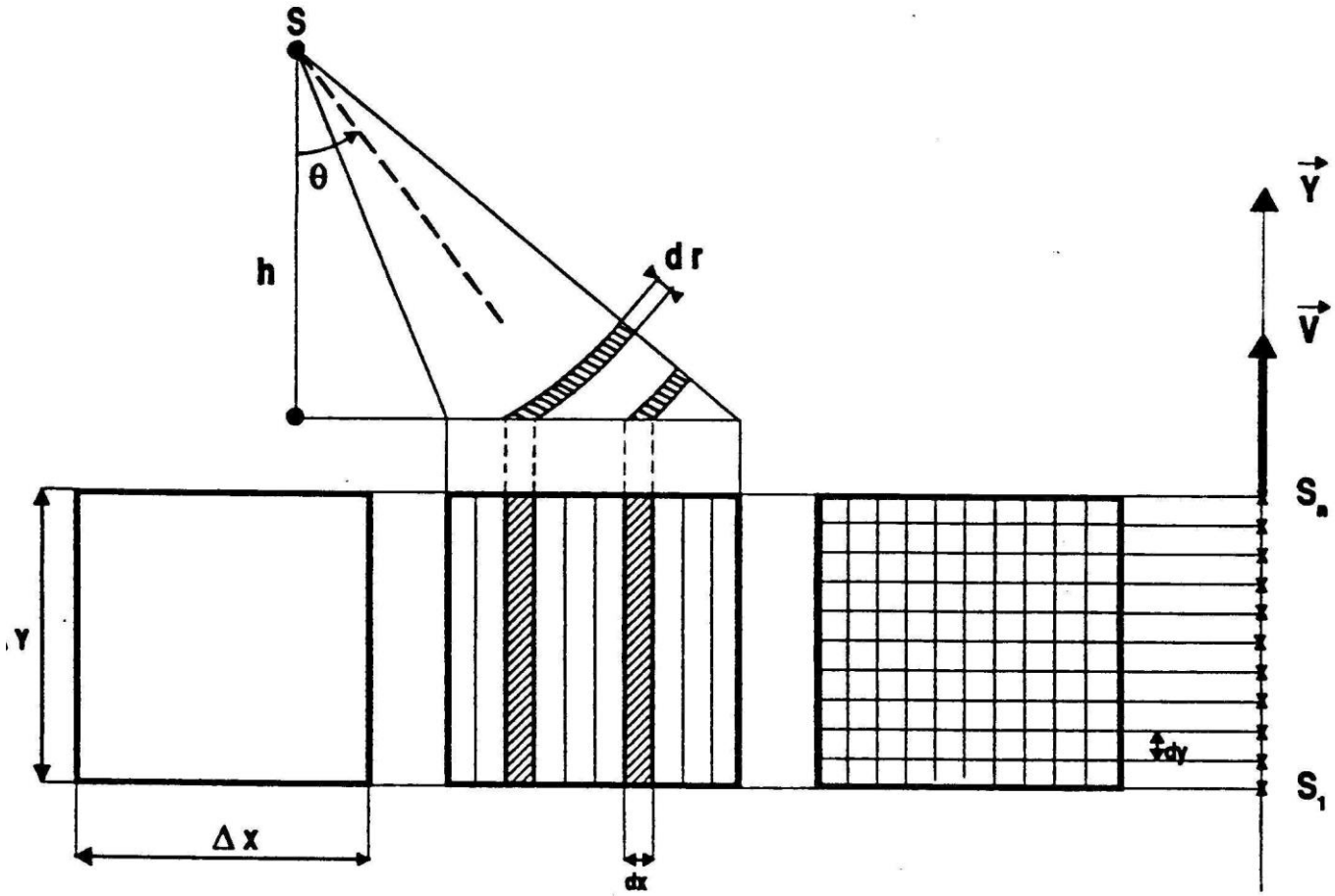

Illustration des gains en résolution, successivement en site et en azimut, apportés par le radar à ouverture de synthèse.

SAR image

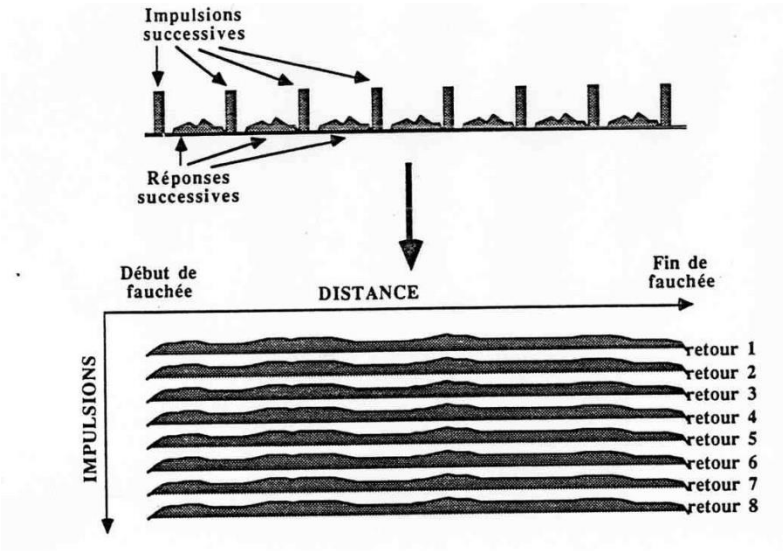
Impulsions successives
Réponses successives
Début de fauchée
DISTANCE
Fin de fauchée
IMPULSIONS
retour 1
retour 2
retour 3
retour 4
retour 5
retour 6
retour 7
retour 8

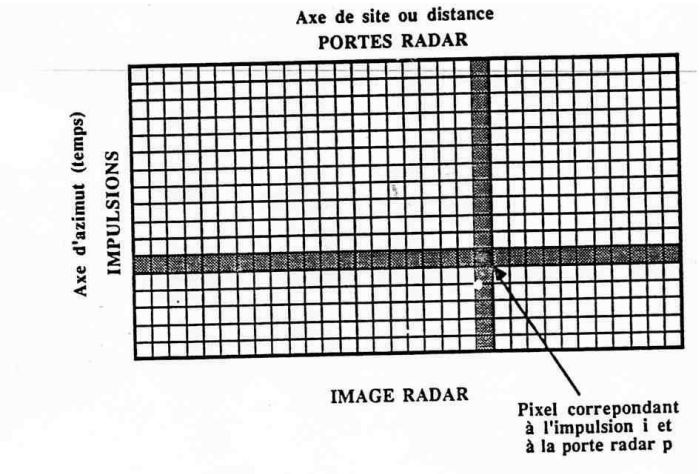
Axe de site ou distance
PORTES RADAR
Axe d'azimut (temps)
IMPULSIONS
IMAGE RADAR
Pixel correpondant à l'impulsion i et à la porte radar p

Spatial resolution

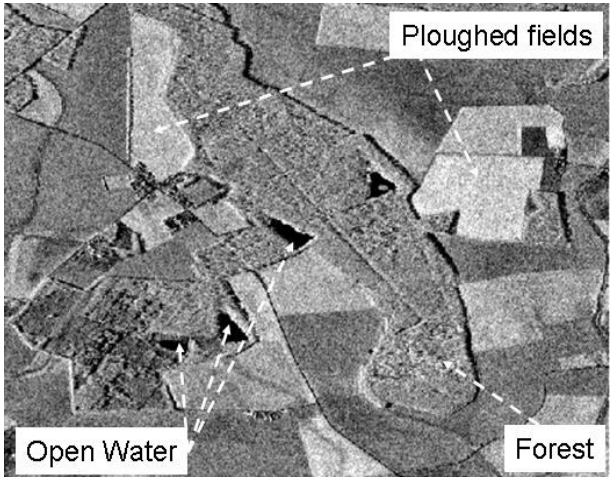

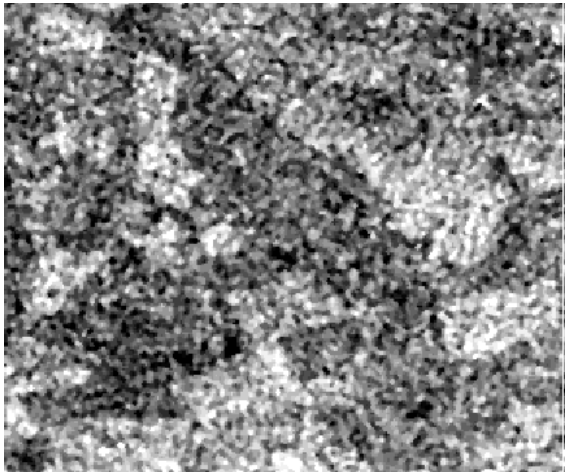

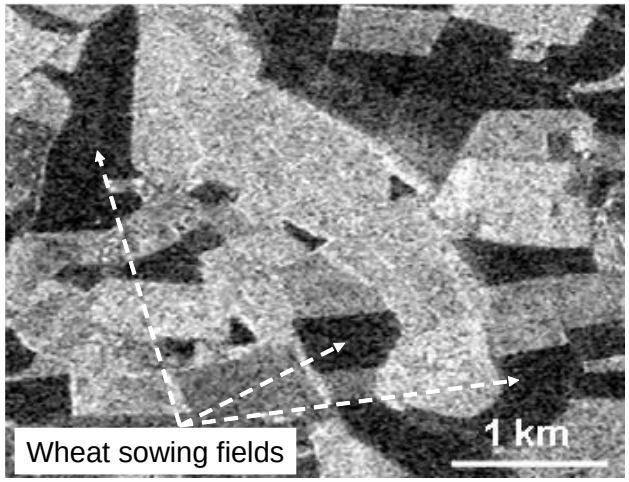

TerraSAR-X ; 12 feb. 2008 ; X band; HH50°; pixel size = 1m
ASAR ; 03 feb. 2008 ;C band; HH23°; pixel size = 12.5m
ALOS/PALSAR ; 12 feb. 2008 ; L band; HH38°; pixel size = 6.25m

Incidence angle

- **Incidence angle**

Refers to the angle between the radar illumination and the normal to the earth's surface.

- **Local incidence angle**

The local incidence angle takes into account the local inclination of the terrain at any point of the image. The local incidence angle determines in part the brightness of the image of each pixel.

Attenuation and speckle

- The attenuation and speckle are the "noise effects" inherent in coherent imaging systems that decrease image quality.

- When a distributed target is observed, the received signal is the coherent (or complex) sum of the elementary signals reflected by many surface elements, all located in the same measuring cell, the rapid phase changes of these elementary signals generate A multiplicative noise when the resulting signal is detected in amplitude or in power.

Speckle origin

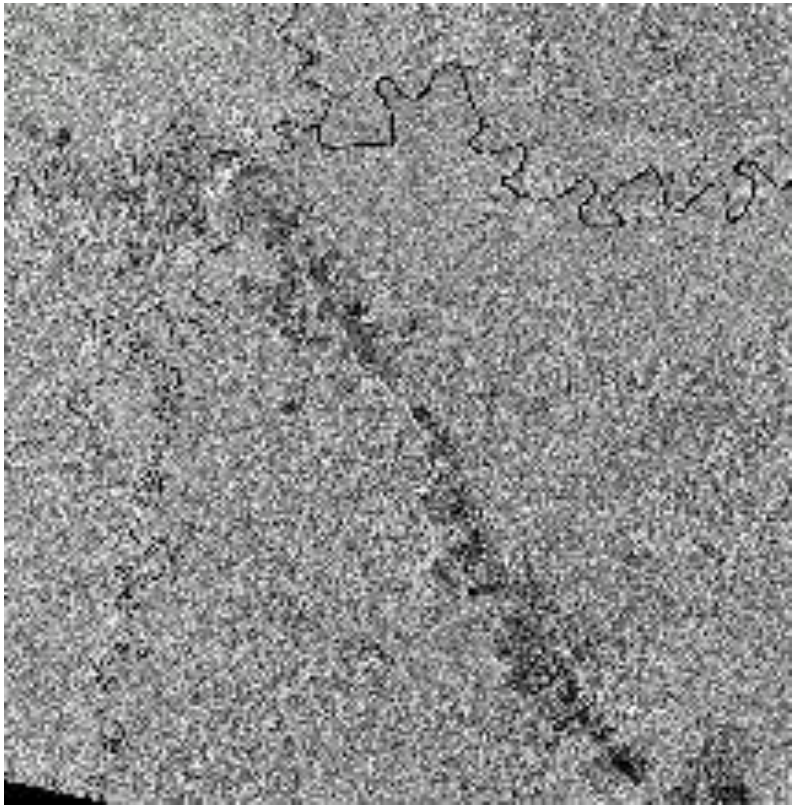

Constructive and destructive local interference takes on the appearance of light and dark spots: the speckle.

Chatoiement

Interférence constructive

Ondes radar cohérentes

Interférence destructive

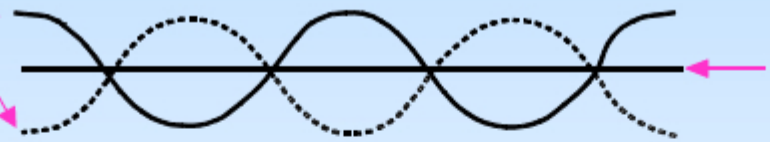

Exemple d'une cible homogène

Interférence constructive

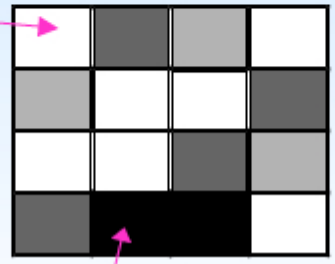

Différents niveaux d'interférence (de constructive à destructive)

Interférence destructive

Radar image

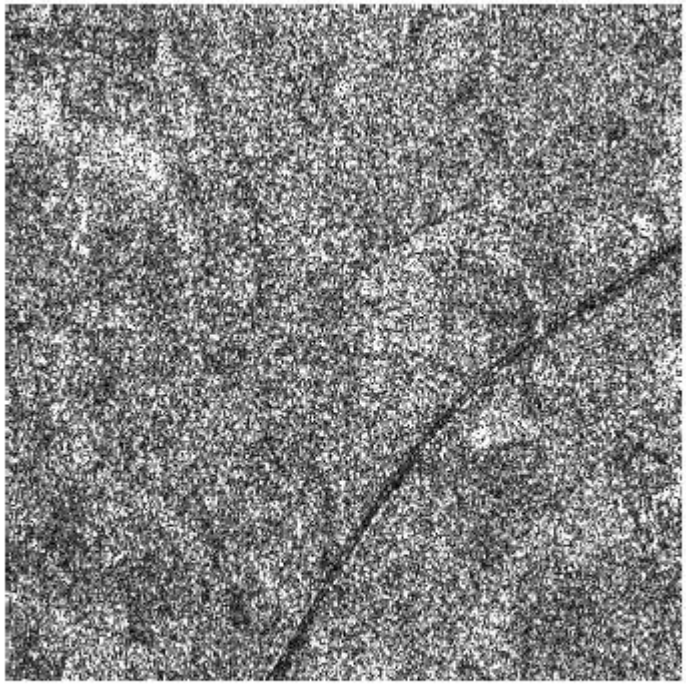

Amplitude image

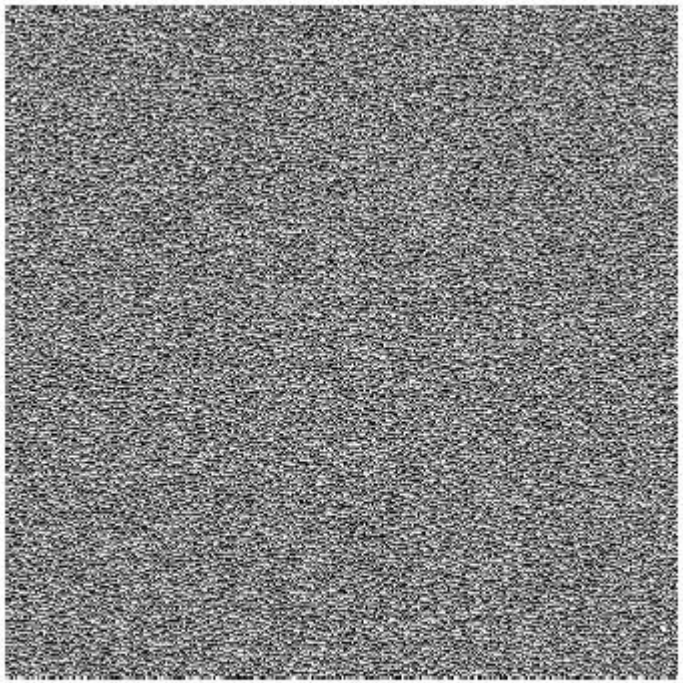

Phase image

RADARSAT I, SLC image

Histogram over an homogeneous area

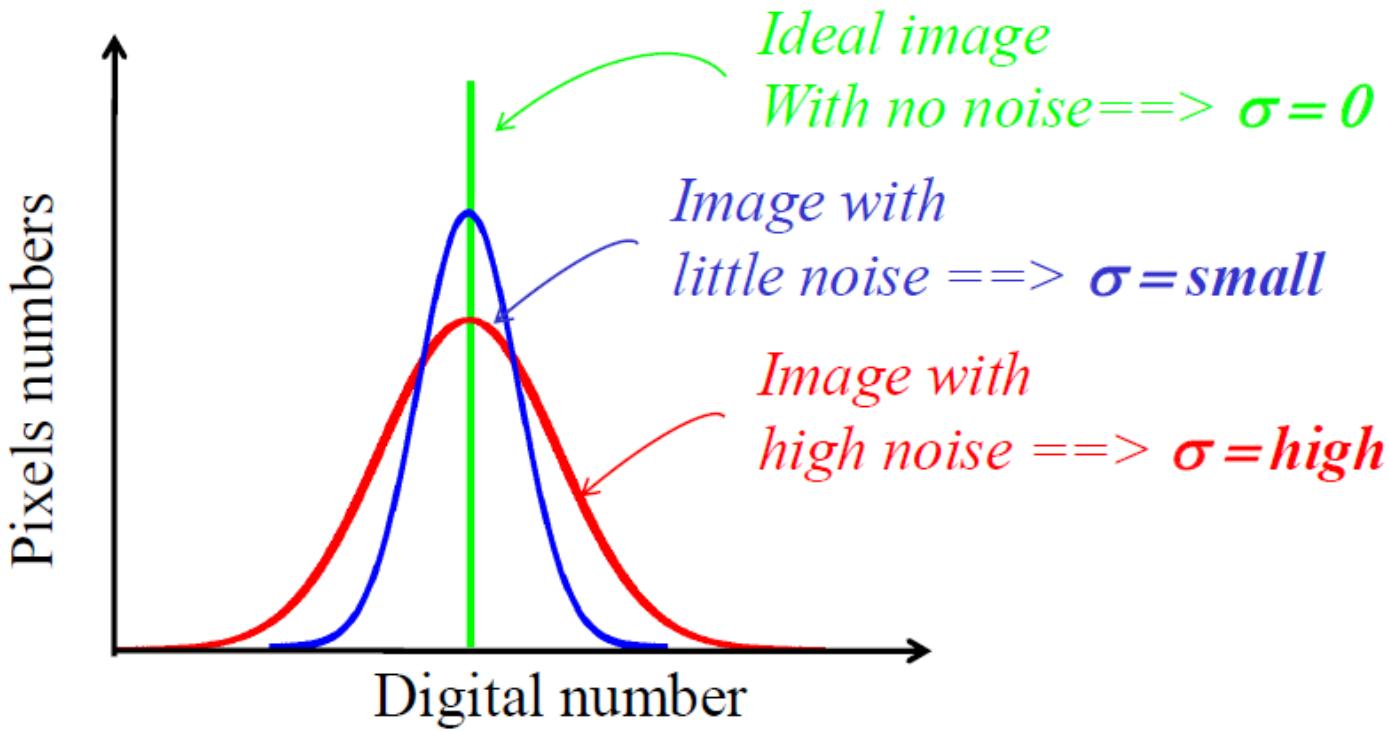

Goal of radar filtering
Decrease of the standard deviations (noise) without modify the mean m (≈radar refelctivity)

Generation of multi-look images

Reduce the noise(speckle) = average pixels (intensity)

In spatial domaine:

*Spatial convolution: image * window*

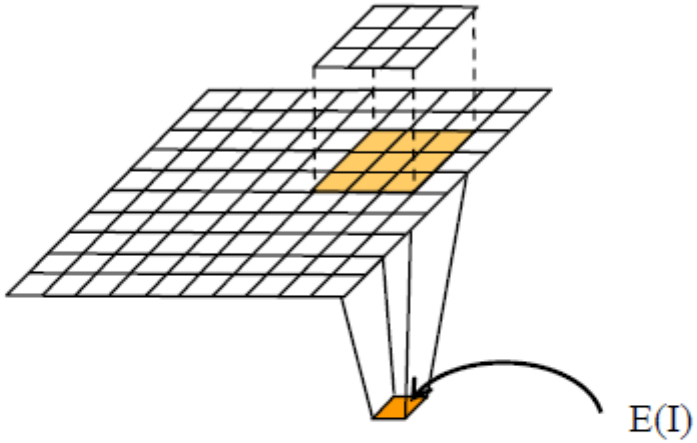

9 looks if pixel sare not correlated

Example: ERS data - PRI products : ≅ 3 looks

SPATIAL MULTILOOK PROCESSING

Sète - France: 21.06.2001 - RADARSAT FINE 1 - INCIDENCE 38°, 9 x9 m

3x1 average window

< 3 Look

Due to pixels correlation!

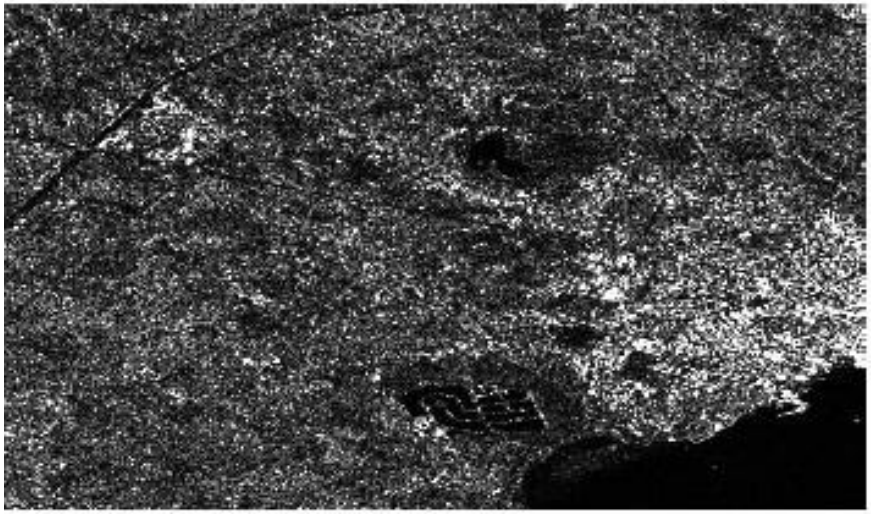

6x2 average window

< 12 Look

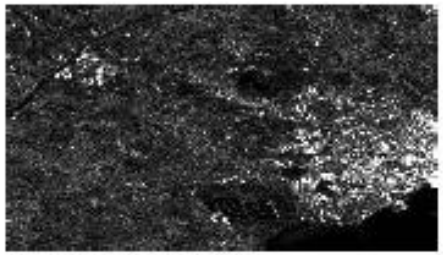

Photo aérienne (www.géoportail.fr)

SAR Image Filtering:

Goal: estimate R $\cong \sigma^{\circ}$

Most simple: Box Filtering: I $\longleftrightarrow$ ***average*** : E(I)

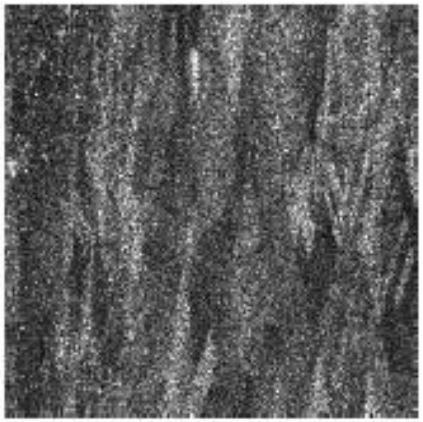

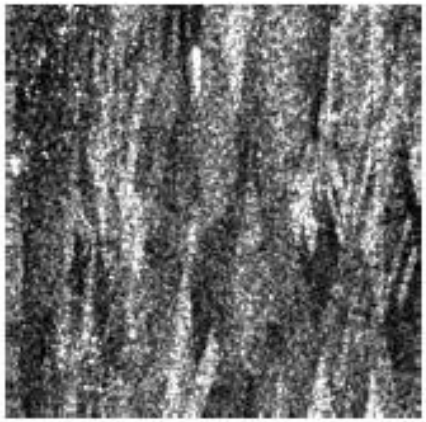

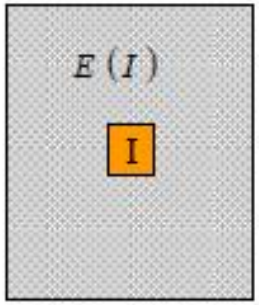

Advantages: simple + best estimation ***(MMSE)*** over homogeneous area

Inconvenients: Details lost, fuzzy introduction

Other classical filters: (median, Sigma, math. morph…..): WORST!

==> Need to introduce specific filters taken into account speckle statistics

Neighbourhood size depends on local scene characteristics
==> ***Adaptive filters***

Adaptative Filter: Frost, Kuan, Lee

homogeneous area:

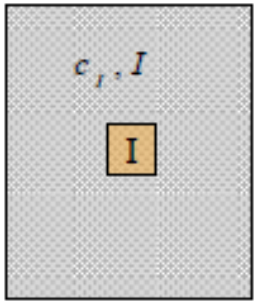

Average over the local window

heterogeneous area:

Keep the central pixel value
(no filtering)

Adaptative Filter: Frost, Kuan, Lee

homogeneous area:

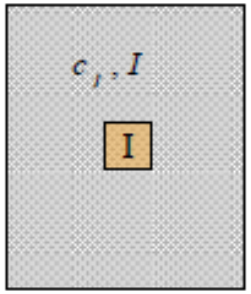

Average over the local window

heterogeneous area:

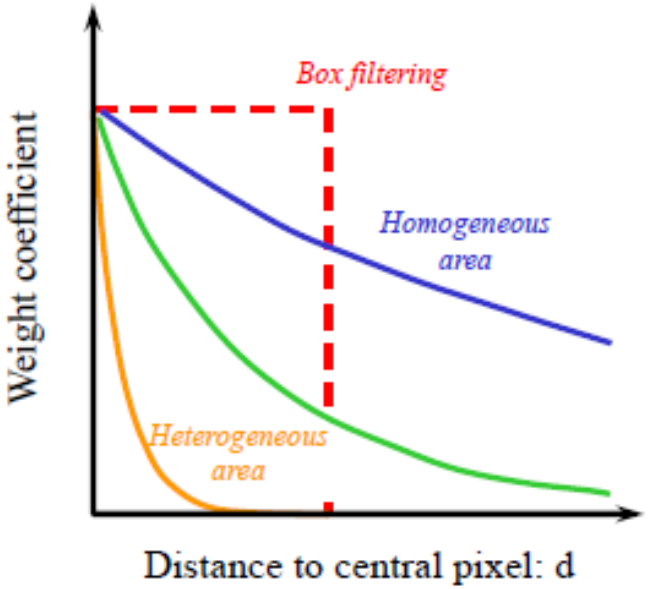

Spatial filtering tools test (3/4)

➔ Comparison of different adaptive filters

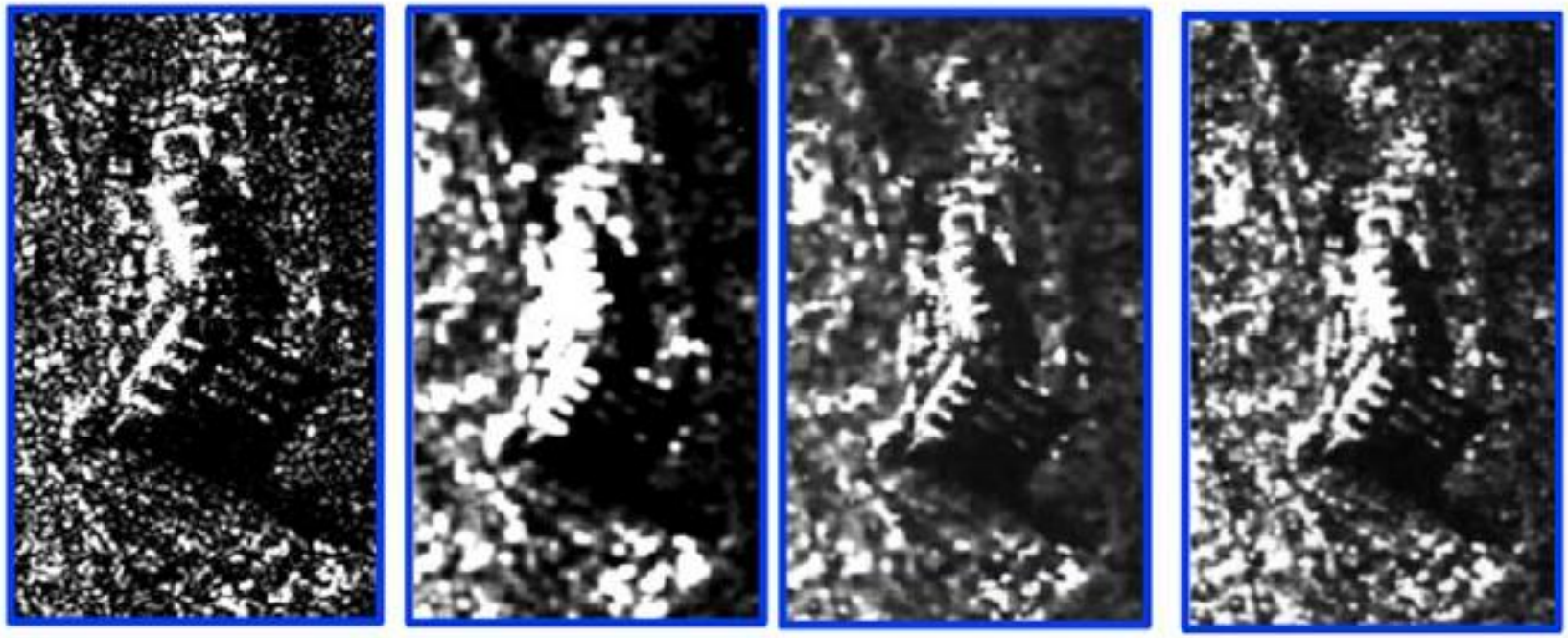

Original image | average 7x7 | Frost 7x7 | Gamma-Gamma MAP 7x7

Radarsat 1 extract, fine mode, 'Salon de Provence'

Simple average computed from the numerical values of neighbor pixels

Generation of multilook images

Reduce speckle: doing the average of pixels (intensity)

In the spatial domain

*Spatial convolution: image * window*

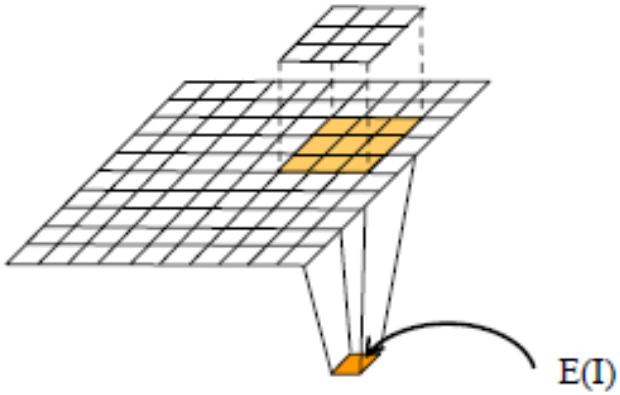

9 looks if pixel sare not correlated

Example: ERS data - PRI products : ≅ 3 looks

Loss of spatial informations (details)

In the temporal domain

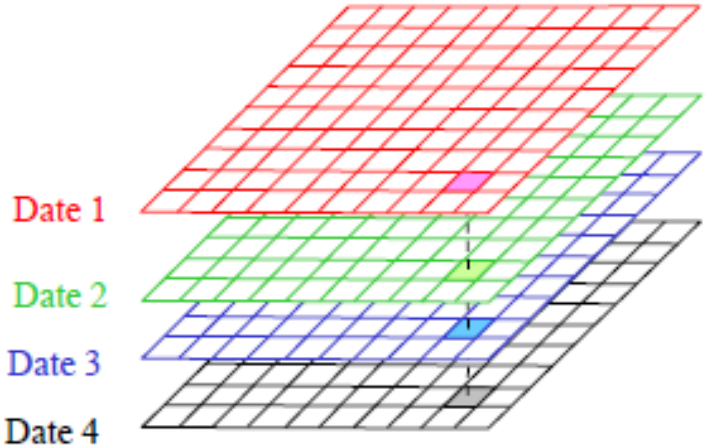

4 looks if surface
has not changed

Loss of temporal informations

: Spatio-temporal domain

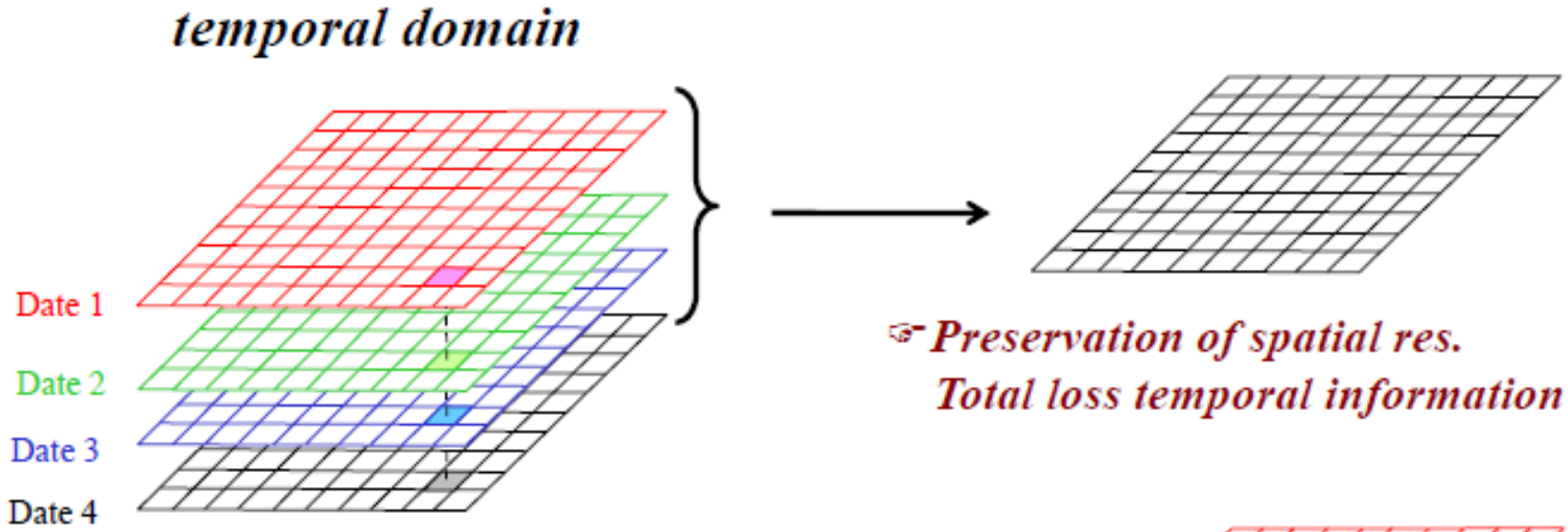

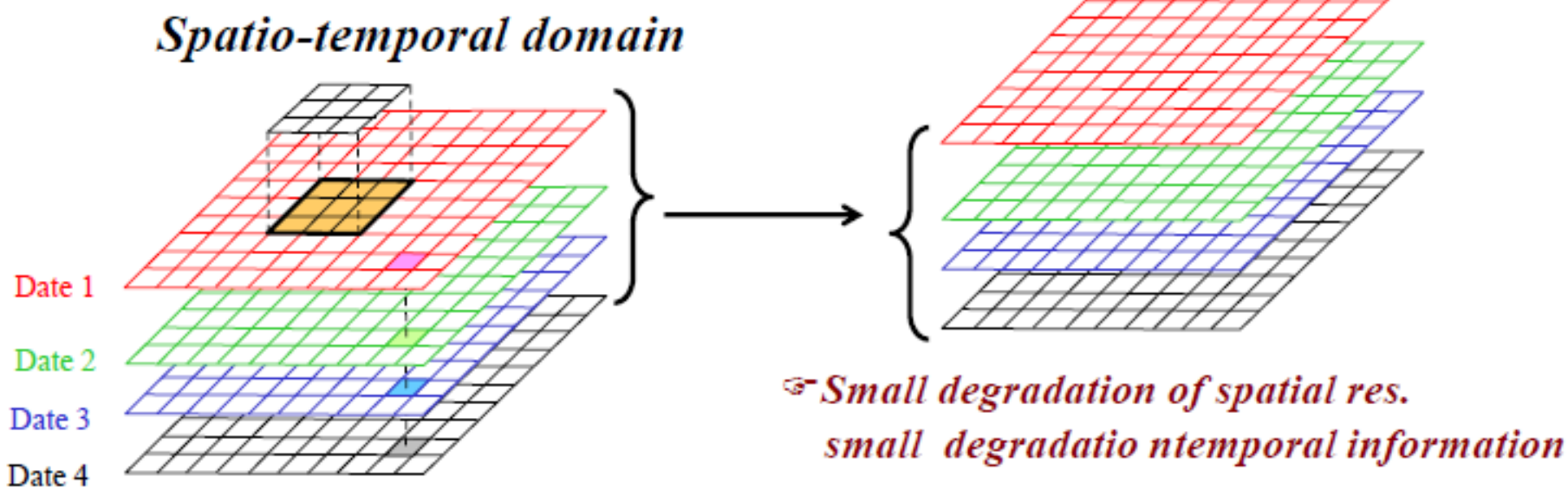

: Spatio-temporal domain

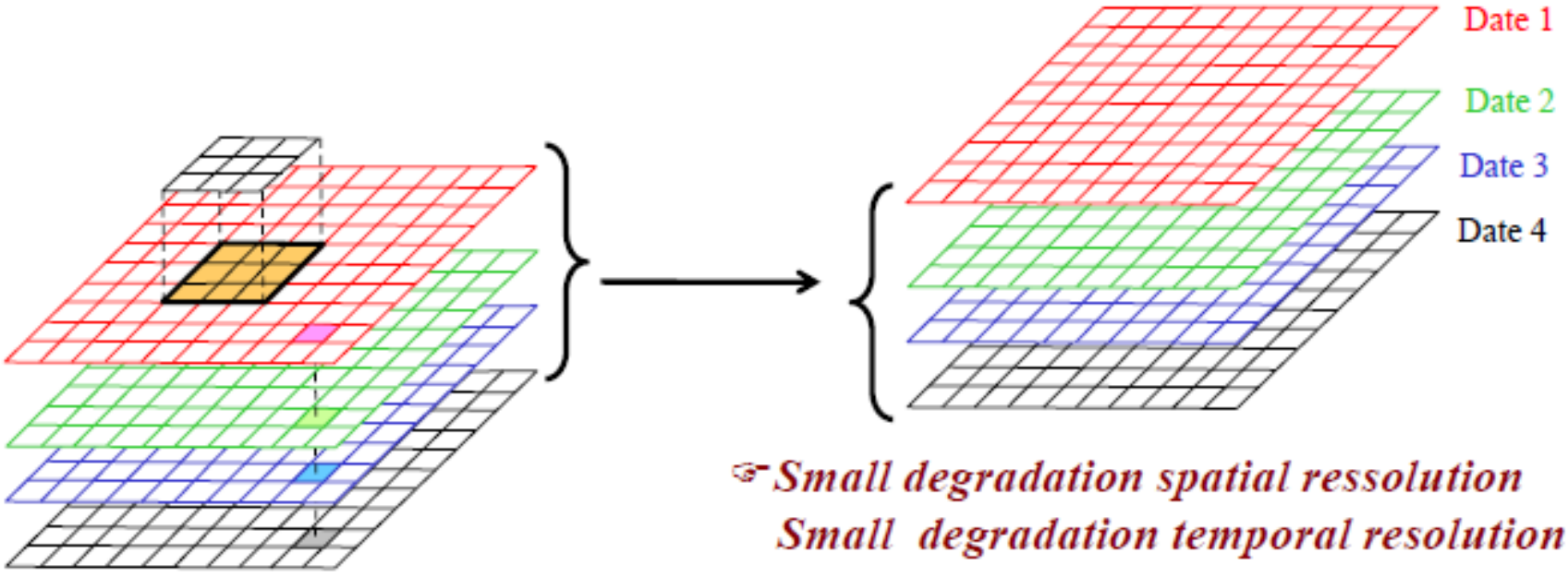

☞ *Small degradation spatial ressolution*
Small degradation temporal resolution

$$J_k = \frac{\langle I_k \rangle}{N} \sum_{i=1}^{N} \frac{I_i}{\langle I_i \rangle} \quad \text{for } k = 1, \ldots, N$$

temporal average

N: acquisitions number (different dates)
J_k: pixel value of the output (filtered) image
I_k: pixel value of acquisition k
$< I_k >$: spatial average over a local neighbor. Around Ik

Ouegan & Yu, IEEE TGRS 20

6) specular and diffuse reflexions

- The roughness of the surface affects the reflectivity of the microwaves and therefore the intensity of the various elements appearing on the radar imagery.
- The smooth horizontal surfaces reflect almost all of the incident waves in a direction opposite to the radar. This type of **reflection is called specular** (from the Latin word speculum which means mirror). Specular surfaces, such as **calm water bodies**, appear as dark areas on radar imagery.
- When microwaves come into contact with a **rough surface**, they are scattered in several directions. This type of interaction is called **diffuse reflection**. The vegetation surfaces produce diffuse reflection.

Scattering

- In general, the scenes observed using an SAR contain two types of reflective surfaces: distributed scatterers and point targets.
- Point targets have a relatively simple geometric shape, like a building. The element usually used to represent point targets is the corner reflector, which results from the quasi-perpendicular intersection of planes (such as the intersection of a paved street and a high building).

Scattering

- Distributed scatterers are regions or surfaces that produce many distinct reflections in different directions. Dissemination from forest cover or cropland are examples of distributed spreaders. The radar captures the portion of the signal that is scattered in the direction of the incident beam.

Surface roughness

- The roughness of a surface as perceived by the radar depends on the wavelength of the signal and the angle of incidence of the beam. In general, a surface is considered smooth if the variations in height of the surface are much smaller than the wavelength of the radar. For a given wavelength, the surface appears to be increasingly rough as the angle of incidence increases. Rough surfaces are usually lighter on radar images than smooth surfaces made of the same material. In general, a rough surface is defined as having variations in height of the order of half the wavelength of the radar.

Rayleigh criterion

$$h^2+L^2=r^2$$

$$hdh=rdr$$

$$\Delta r=h\frac{\Delta h}{r}$$

$$\Delta h\cos\theta=\Delta r$$

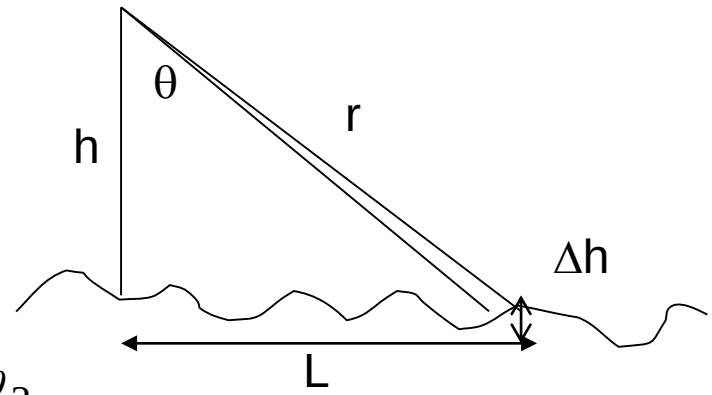

The phase difference is written as: $\Delta\varphi=\frac{2\Delta h\cos\theta}{\lambda}2\pi$

The surface is smooth when $\Delta\varphi=\frac{2\Delta h\cos\theta}{\lambda}2\pi$ is small

s/λ is small (*s*=Δ*h*)

$\cos\theta$ is low

Surface scattering

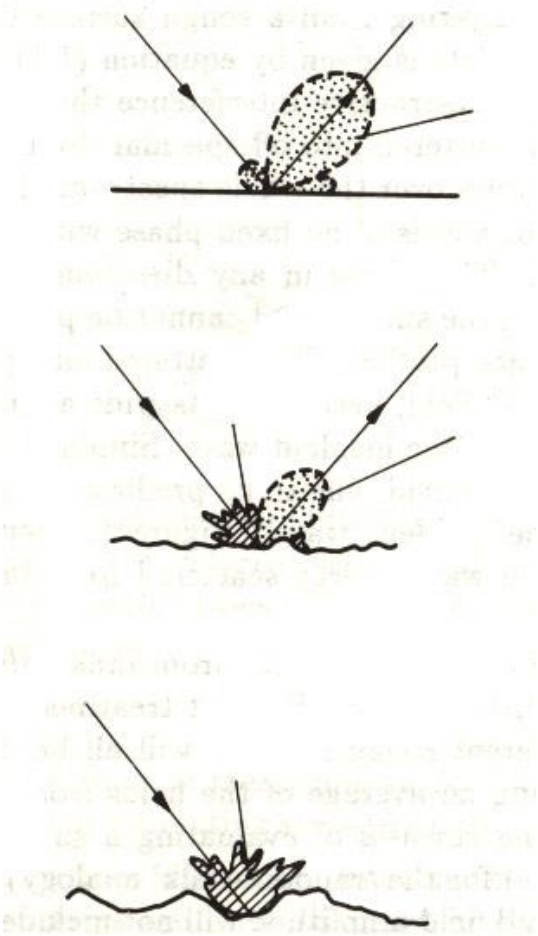

Smooth surface

Meduim rough surface

Rough surface

Surface roughness

$$\langle h \rangle = \int_{-\infty}^{+\infty} hp(h)dh = 0$$

$$\sigma = \sqrt{\langle h^2 \rangle}$$

$$p(h) = \frac{1}{\sigma\sqrt{2\pi}} exp\left(-\frac{h^2}{2\sigma^2}\right)$$

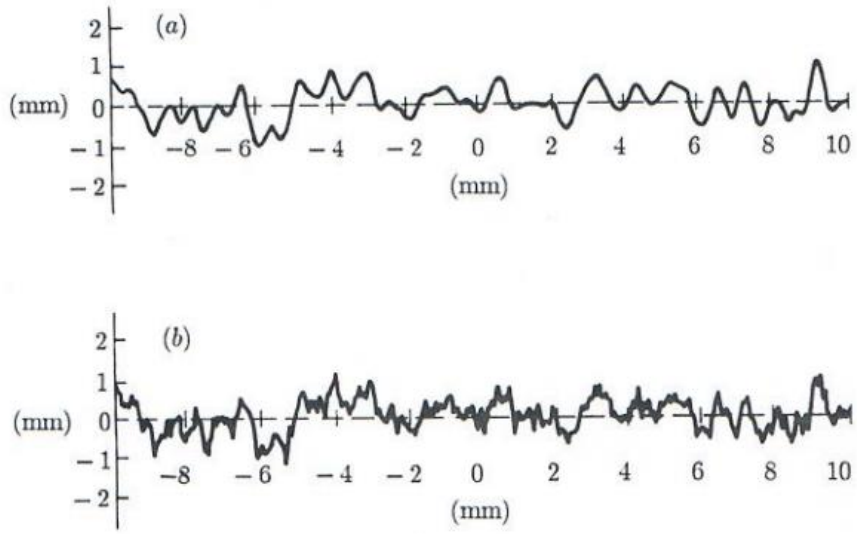

Fonction de corrélation des hauteurs

$$C(R) = \frac{\langle h(r)h(r+R)\rangle}{\sigma^2}$$

$$C(R) = \exp\left(-\frac{R^2}{l^2}\right)$$

$$C(R) = exp\left(-\frac{|R|}{l}\right)$$

$$C(R) = \exp\left\{-\left(\frac{|R|}{l1}\right)\left[1 - exp\left(-\frac{|R|}{l2}\right)\right]\right\}$$

$$C(R) = \exp\left(-\left(\frac{R}{l}\right)^{\alpha}\right)$$

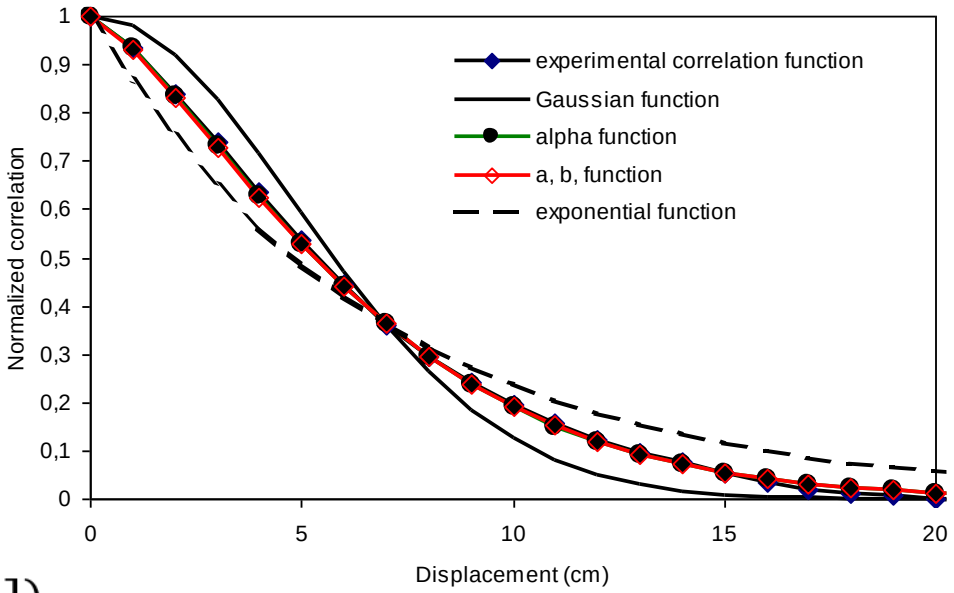

Effect of soil roughness

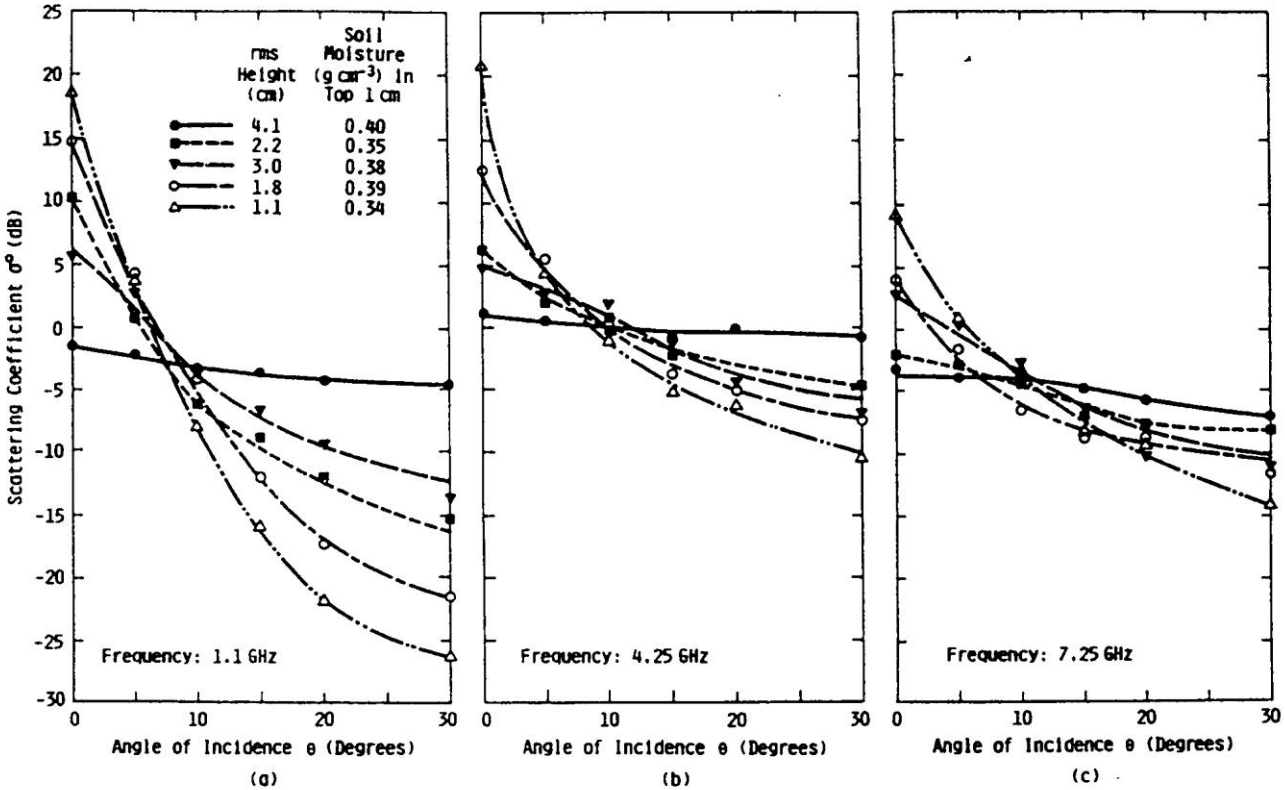

Angular response of the scattering coefficient for five fields with high levels of moisture content at (a) 1.1 GHz, (b) 4.25 GHz, and (c) 7.25 GHz.

Surface roughness

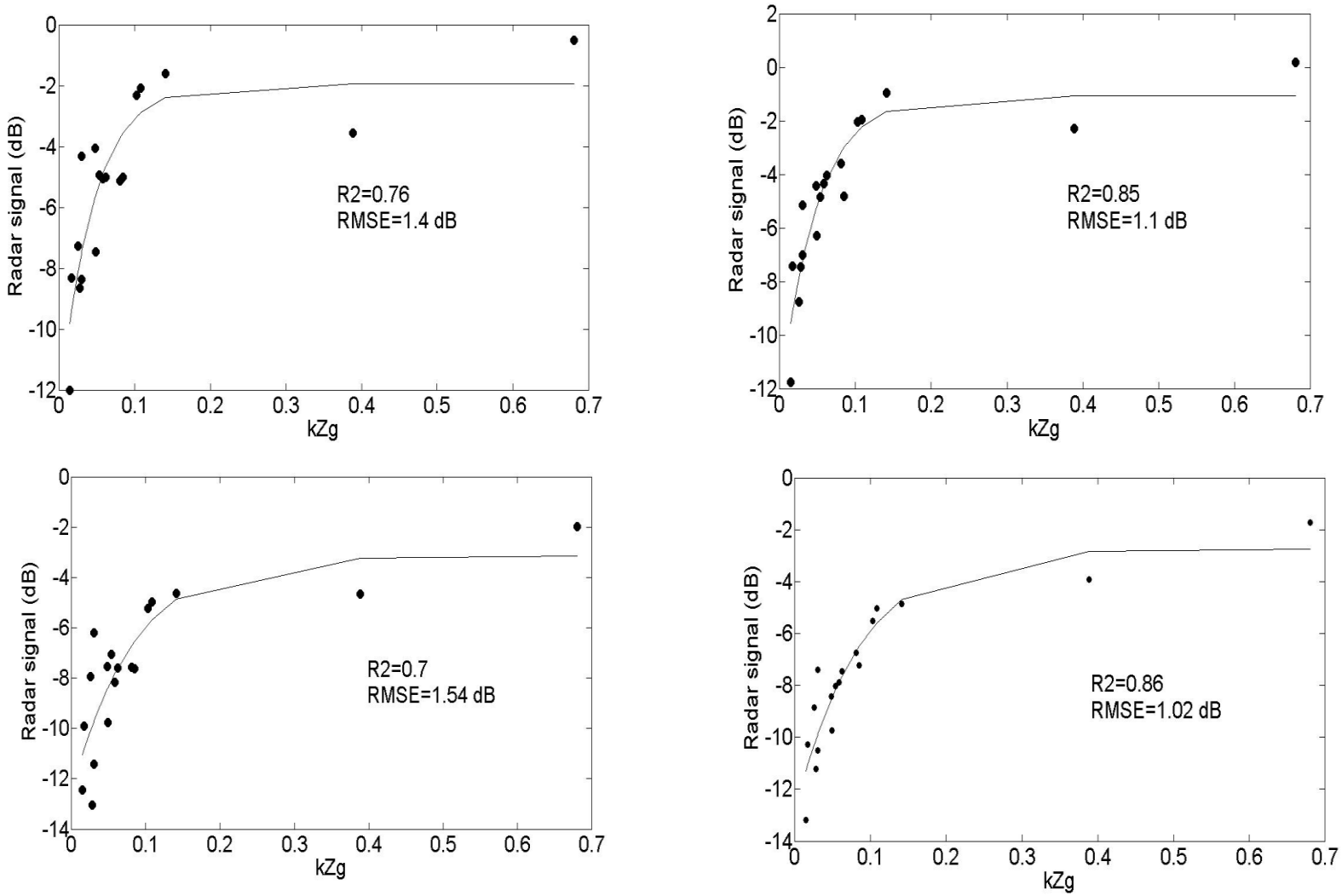

Relationship between *kZg* and measured radar signals, for: a) *HH* pol at 30°, b) *VV* pol at 30°, c) *HH* pol at 35°, d) *VV* pol at 35° (**ERASME** airborne data)

Radar sign

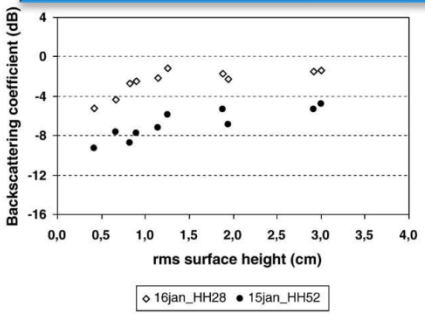

Villamblain – TerraSAR-X (a)

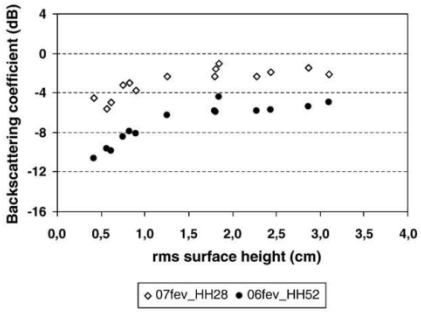

Villamblain – TerraSAR-X (c)

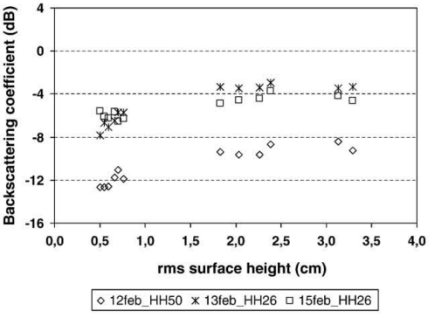

Orgeval – TerraSAR-X (e)

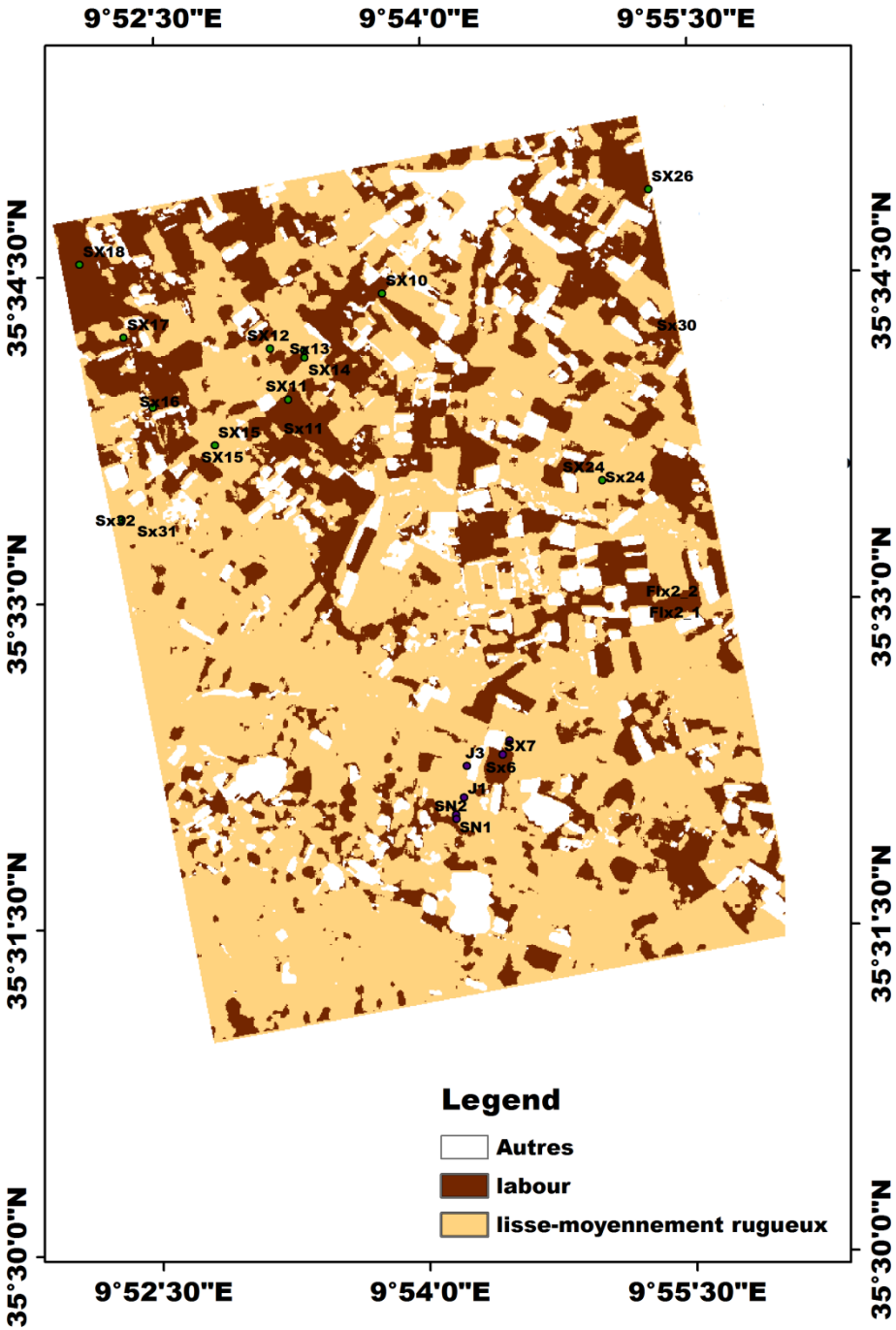

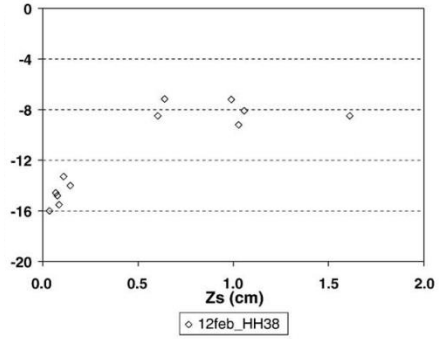

geval – PALSAR (h)

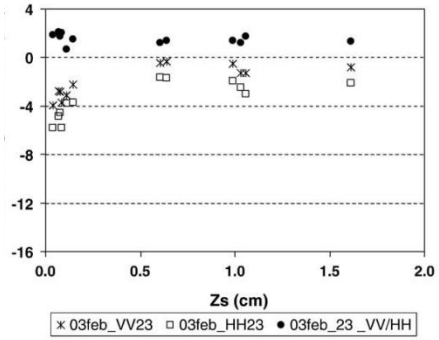

geval – ASAR (j)

ribi et al, RSE, 2008)

Effect of roughne

Effect of roughne

ngle

CESBIO

Soil surface backscattering models

Huygens principals (Stratton Shu Equations)

$$\vec{E}(r) = -\iint i\omega\mu G(\vec{r},\vec{r}')(\vec{n} x \vec{H}(\vec{r}')) + \vec{\nabla} \wedge G(\vec{r},\vec{r}')(\vec{n} \wedge \vec{E}(r') d\vec{r}'$$

IEM

$$\sigma^0{}_{pp} = \frac{k^2}{2}\left|f_{pp}\right|^2 \exp(-4s^2k^2\cos^2\theta)\sum_{n=1}^{+\infty}\frac{\left(4s^2k^2\cos^2\theta\right)^n}{n!}W^{(n)}(2k\sin\theta,0) +$$

$$\frac{k^2}{2}Re\left(f^*{}_{pp}F_{pp}\right)\exp\left(-3s^2k^2\cos^2\theta\right)\sum_{n=1}^{+\infty}\frac{\left(4s^2k^2\cos^2\theta\right)^n}{n!}W^{(n)}(2k\sin\theta,0) +$$

$$\frac{k^2}{8}\left|F_{pp}\right|^2 \exp(-2s^2k^2\cos^2\theta)\sum_{n=1}^{+\infty}\frac{\left(4s^2k^2\cos^2\theta\right)^n}{n!}W^{(n)}(2k\sin\theta,0)$$

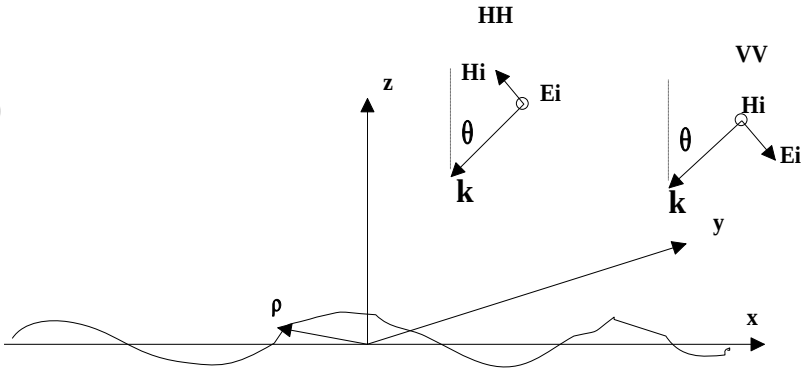

SPM

$$\sigma^0_{pp} = 8k^4s^2\cos^4\theta\left|\alpha_{pp}\right|^2 W(2k\sin\theta,0)$$

Numerical, analytical physical, semi-empirical, empirical modelings

SPM/ Domaine de validité :

Surface lisse de faible écart type des pentes

ks<0.3 et *kl*<3

m<0.3

m : Ecart type des pentes.

Coefficient de rétrodiffusion :

$$\sigma_{pp}^{0} = 8k^4 s^2 \cos^4\theta \left|\alpha_{pp}\right|^2 W(2k\sin\theta, 0)$$

$$\sigma_{vh}^{0} = \sigma_{hv}^{0} = \left[\pi k^4 s^4 \cos^2\theta \frac{\left|(\varepsilon_r - 1)(R_{//} - R_{\perp})\right|^2}{2}\right]$$

$$\times \int \int_{-\infty}^{+\infty} \frac{u^2 v^2}{\left|D_0\right|^2} W(u - k\sin\theta, v)\, W(u + k\sin\theta, v)\, du dv$$

$$W(u,v) = \frac{1}{2\pi} \int \int_{-\infty}^{+\infty} \rho(x,y)\, e^{-jux - juy} dx\, dy$$

$$\alpha_{hh} = R_{\perp}$$

$$\alpha_{vv} = (\varepsilon_r - 1) \frac{\sin^2\theta - \varepsilon_r (1 + \sin^2\theta)}{\left[\varepsilon_r \cos\theta + \sqrt{\varepsilon_r - \sin^2\theta}\right]^2}$$

$$D_0 = \sqrt{k'^2 - u^2 - v^2} + \varepsilon_r \sqrt{k^2 - u^2 - v^2}$$

BACKSCATTERING MODELS VALIDATION

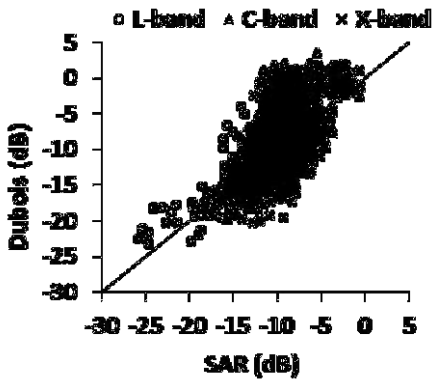

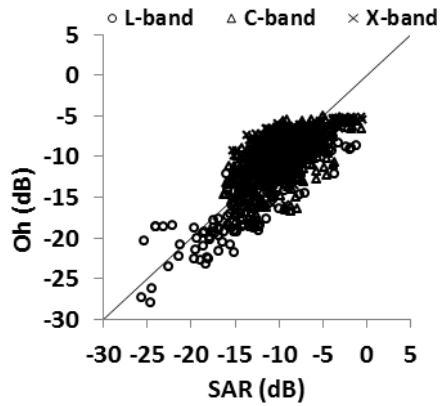

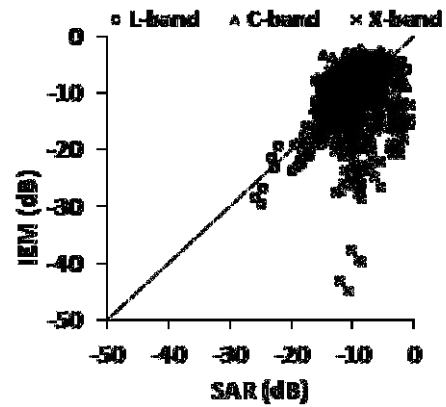

$$\sigma^{\circ}_{HH} = 10^{-1.287}(\cos\theta)^{1.227}\ 10^{0.009\,cotan(\theta)\,mv}\ (k\,Hrms)^{0.86\,sin\,(\theta)}$$

$$\sigma^{\circ}_{VV} = 10^{-1.138}(\cos\theta)^{1.528}\ 10^{0.008\,cotan(\theta)\,mv}\ (k\,Hrms)^{0.71\,sin\,(\theta)}$$

$$\sigma^{\circ}_{HV} = 10^{-2.325}(\cos\theta)^{-0.01}\ 10^{0.011\,cotan(\theta)\,mv}\ (k\,Hrms)^{0.44\,sin\,(\theta)}$$

Gorrab et al., 2015, Chokr et al., 2016,

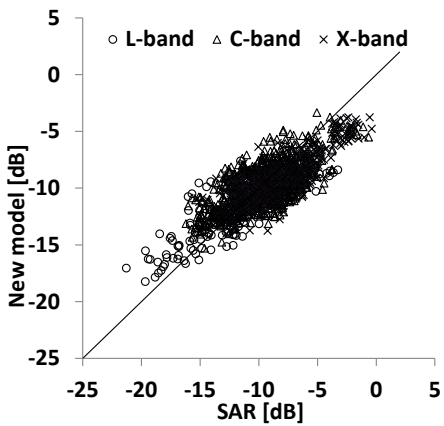

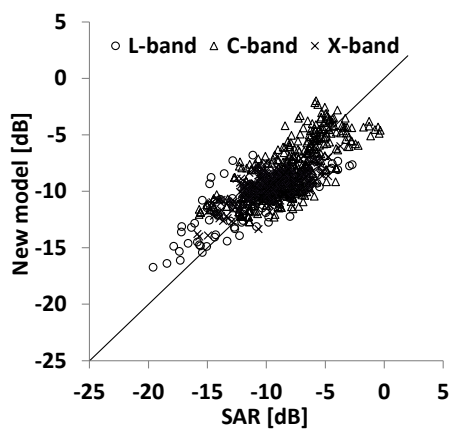

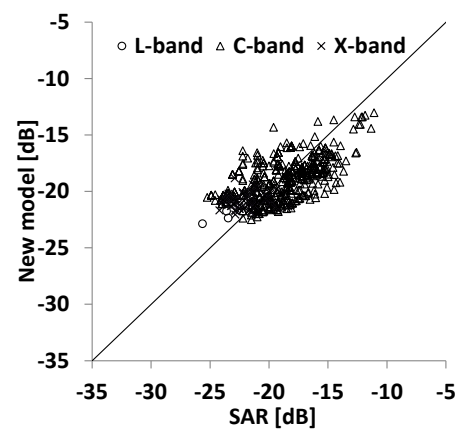

N. Baghdadi, M. Chokr, M. Zribi, Remote Sensing, 2016

Effect of soil moisture

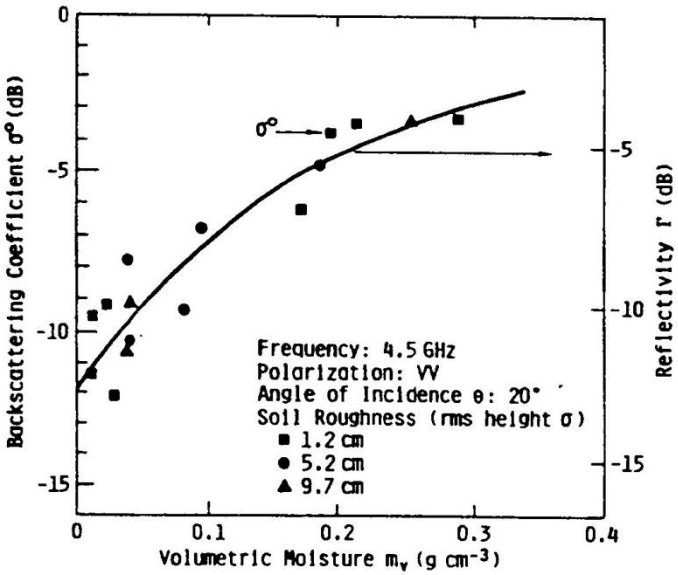

Measured scattering coefficient σ° (left scale) as a function of soil-moisture content for three surface roughnesses. The solid curve is the reflectivity Γ (right scale) calculated on the basis of dielectric measurements (from LeToan, 1982).

Volume scattering

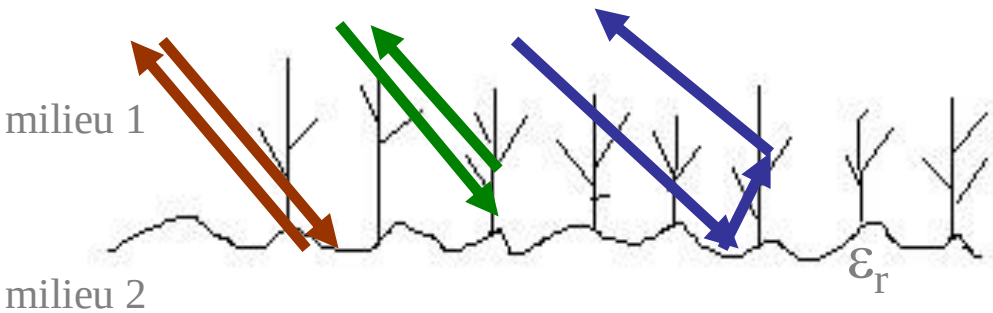

$$\sigma^0_{total} = \sigma^0_{veg} + \sigma^0_{sol-veg} + \gamma^2(\theta)\sigma^0_{sol}$$

Vegetation scattering

Multiple scattering soil-vegetation

Soil scattering attenuated with vegetation

Sentinel-1 signal modeling

- **Vegetated cover soil (WCM):**

$$\sigma^0_{tot} = \sigma^0_{veg} + T^2 \sigma^0_{sol}$$

$$\sigma^0_{veg} = A.V_1.\cos\theta \ (1- T^2)$$

$$T^2 = \exp(-2.B.V_2.\sec\theta)$$

σ^0_{soil} = computed using the IEM or other models

(Attema and Ulaby 1978)

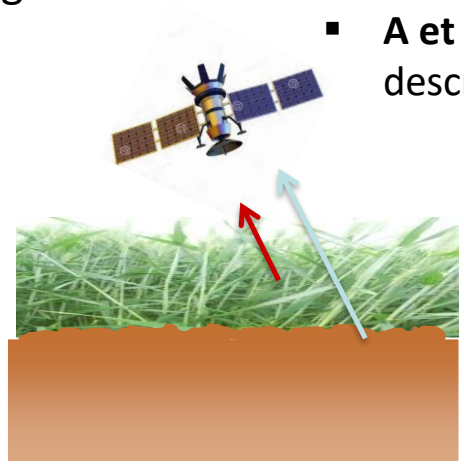

- σ^0_{tot} **:** backscattered radar signal (linear unit)
- $\boldsymbol{\sigma^0_{veg}}$ **:** Vegetation contribution (linear unit)
- $\mathbf{T^2}$ **:** Attenuation
- $\boldsymbol{\sigma^0_{sol}}$ **:** Soil contribution (linear unit)
- $\mathbf{V_1 = V_2}$ **:** vegetation descriptors (BIO (kg/m2), VWC (kg/m2), HVE (m), LAI (m2/m2), FAPAR, FCOVER, and NDVI)
- $\boldsymbol{\theta}$ **:** Incidence angle
- **A et B:** fitting parameters depend on vegetation descriptors and radar configuration

In Situ measurements

Parameters:

- -Soil moisture
- -Roughness
- -Vegetation cover height
- -Leaf Area Index (LAI)

WCM parametrization

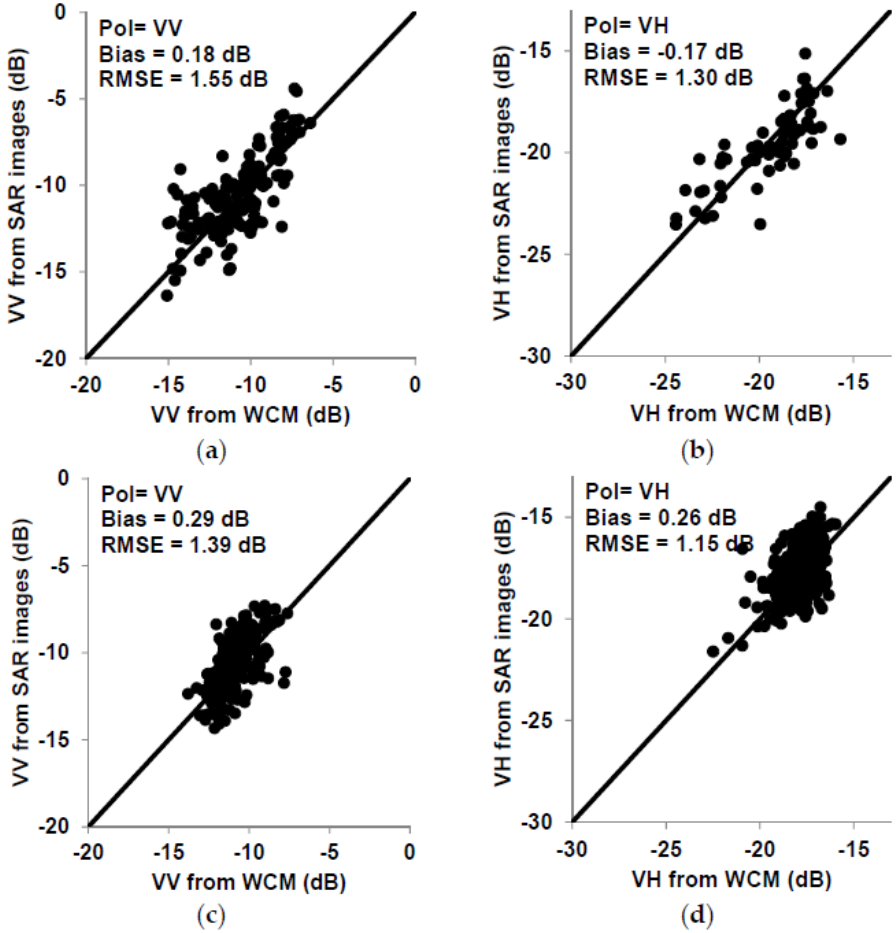

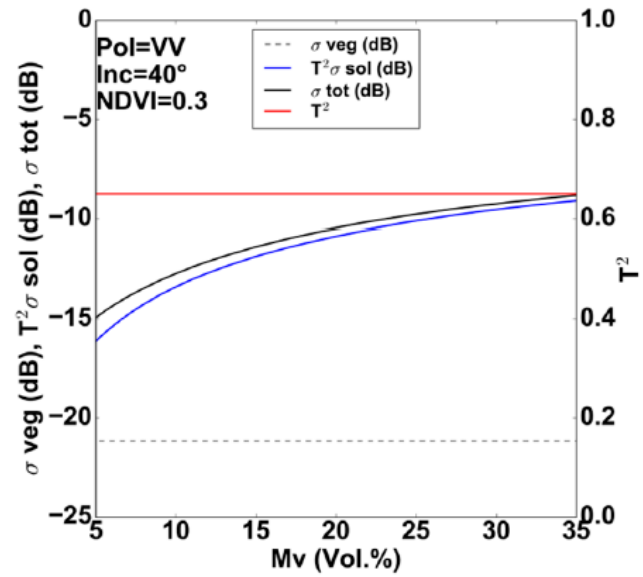

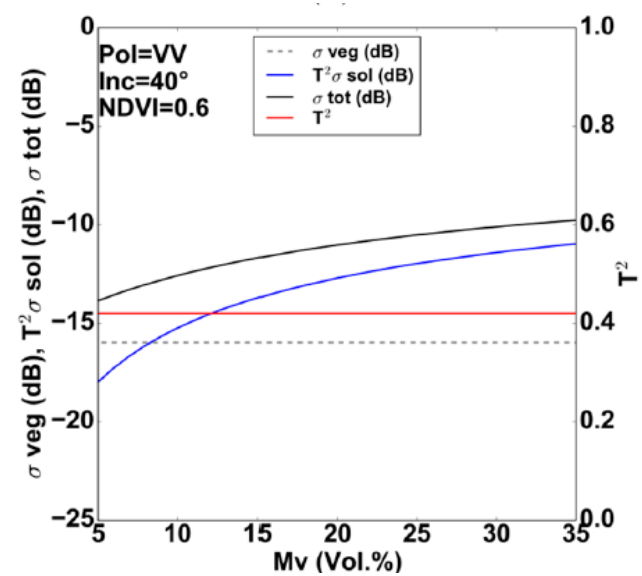

Baghdadi et al., 2017, RS, Bousbih et al., 2017, sensors

Soil moisture maps by coupling S1&S2

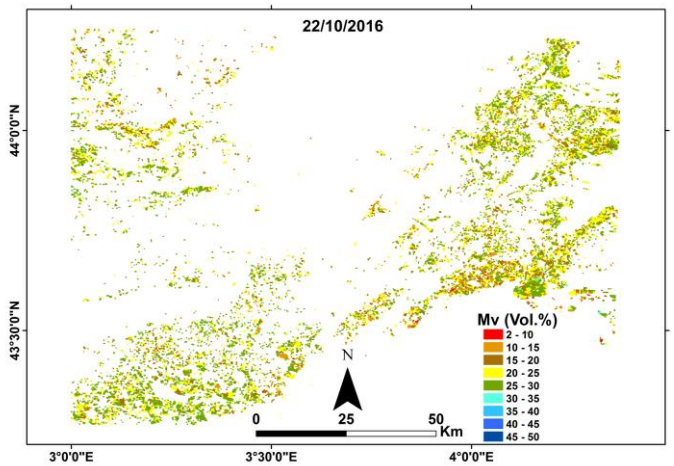

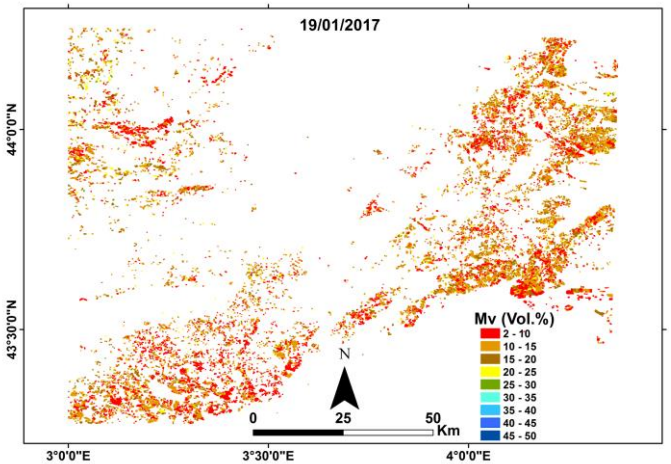

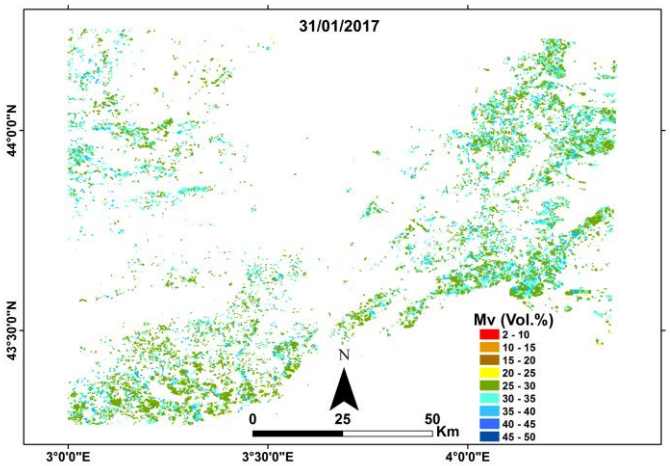

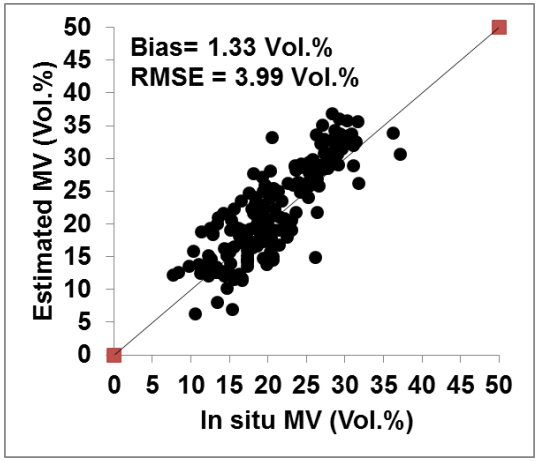

- **Soil moisture maps over Occitanie region (2016-2018, Time : 6 days, plot scale)**
- **The used S2 images are in surface reflectance ➔ generated using MAJA-Theia software (http://www.theia-land.fr/fr/produits/r%C3%A9flectance-sentinelle-2)**
- **Agricultural zones were extracted from the land cover map produced by the ScientificExpertise Center on land cover (SEC OSO)**

Sol moisture mapping(2), synergie radar/optical RS(ASAR, SPOT-VGT)

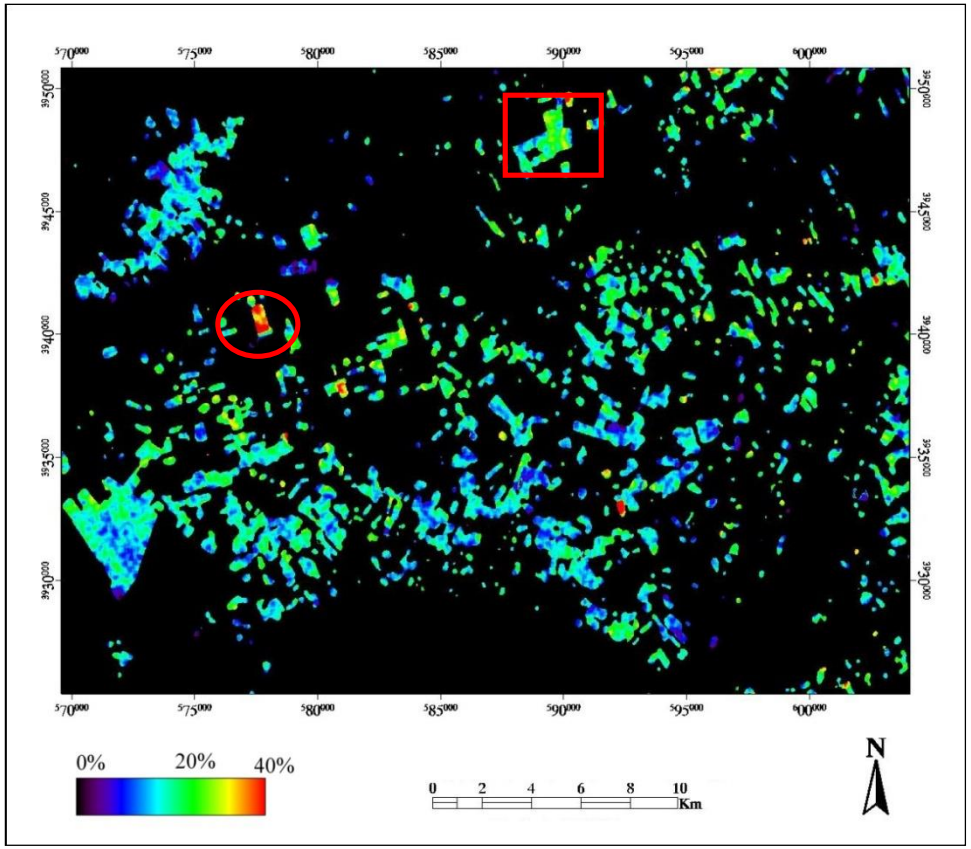

Cereals soil moisture mapping, identification of irrigated areas 07/03/2009

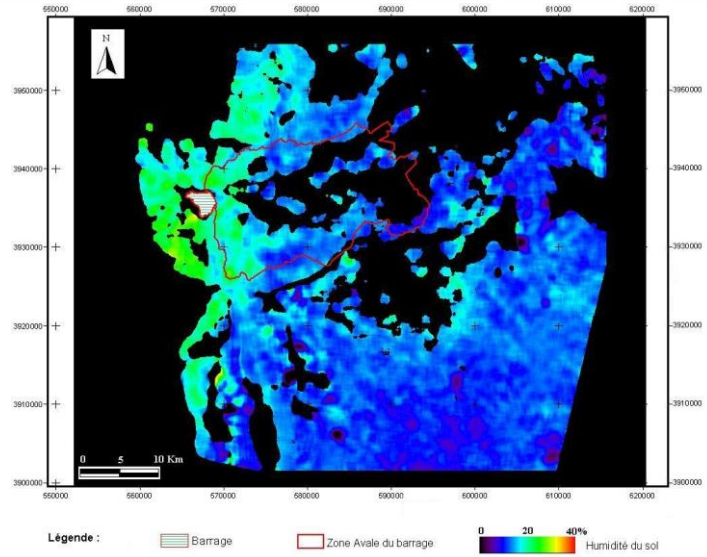

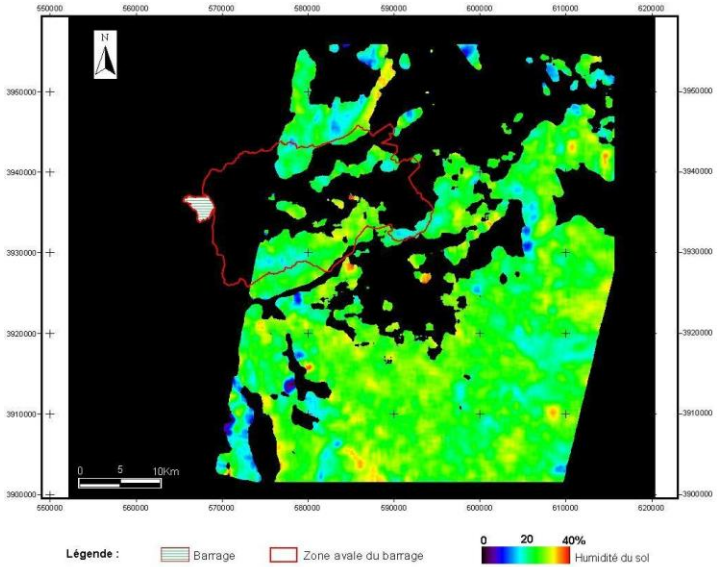

(Zribi et al., HESS, 2011) **Moisture mapping over olive groves at 11/04/2009 and 12/04/2009.**

Radar polarimetry

1) Radar polarimetry

Radar polarimetry is the science of acquisition, processing and analysis of the polarization of an electromagnetic field.

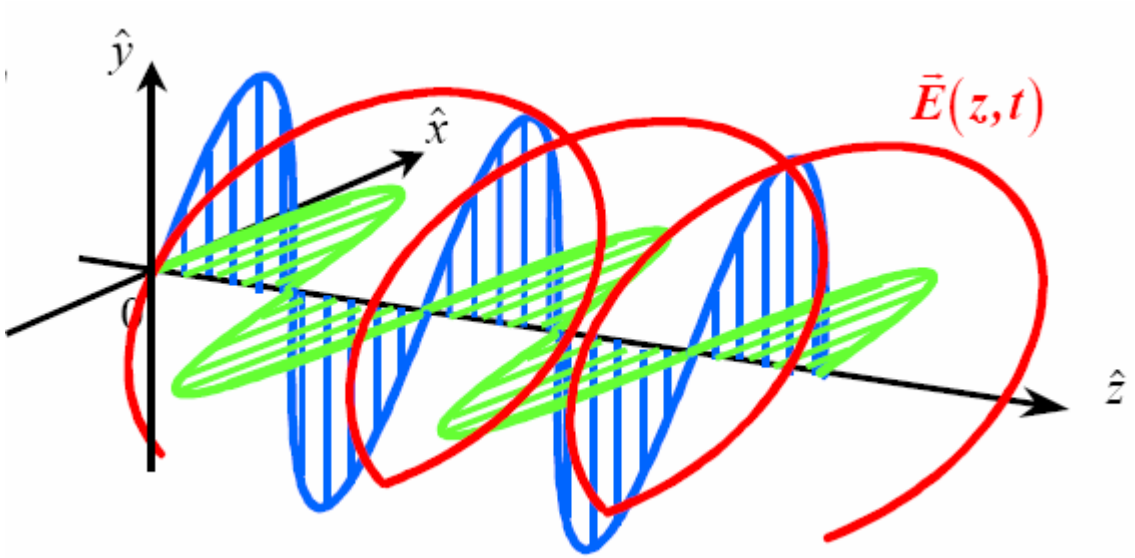

JONES MATRIX OR SCATTRING MATRIX

$$\begin{bmatrix} E_X^S \\ E_Y^S \end{bmatrix} = \frac{e^{jkr}}{r} \begin{bmatrix} S_{XX} & S_{XY} \\ S_{YX} & S_{YY} \end{bmatrix} \begin{bmatrix} E_X^i \\ E_Y^i \end{bmatrix}$$

Defined in local coordinates of the system

[S] is independent of the state of polarization of the incident wave

[S] is dependent on frequency and geometry and dielectric properties of the scatterer

TOTAL SCATTERED POWER

$$Span([S]) = Trace\left([S][S]^{T*}\right)$$
$$= |S_{XX}|^2 + |S_{XY}|^2 + |S_{YX}|^2 + |S_{YY}|^2$$

POLARIMETRIE RADAR

$$[S]=\frac{e^{jkr}}{r}\begin{bmatrix} S_{XX} & S_{XY} \\ S_{YX} & S_{YY} \end{bmatrix}=\frac{e^{jkr}}{r}\underbrace{\begin{bmatrix} |S_{XX}|e^{j\varphi_{XX}} & |S_{XY}|e^{j\varphi_{XY}} \\ |S_{XY}|e^{j\varphi_{XY}} & |S_{YY}|e^{j\varphi_{YY}} \end{bmatrix}}_{\text{ABSOLUTE BACKSCATTERING MATRIX}}$$

$$[S]=\underbrace{\frac{e^{jkr}e^{j\varphi_{XX}}}{r}}_{\text{Absoluate phase factor}}\underbrace{\begin{bmatrix} |S_{XX}| & |S_{XY}|e^{j(\varphi_{XY}-\varphi_{XX})} \\ |S_{XY}|e^{j(\varphi_{XY}-\varphi_{XX})} & |S_{YY}|e^{j(\varphi_{YY}-\varphi_{XX})} \end{bmatrix}}_{\text{RELATIVE BACKSCATTERING MATRIX}}$$

Five parameters: 3 amplitudes and 2 phases

POLARIMETRIC DIMENSION OF SCATTERERS:5

Sinclair Color Coding

© Google Earth

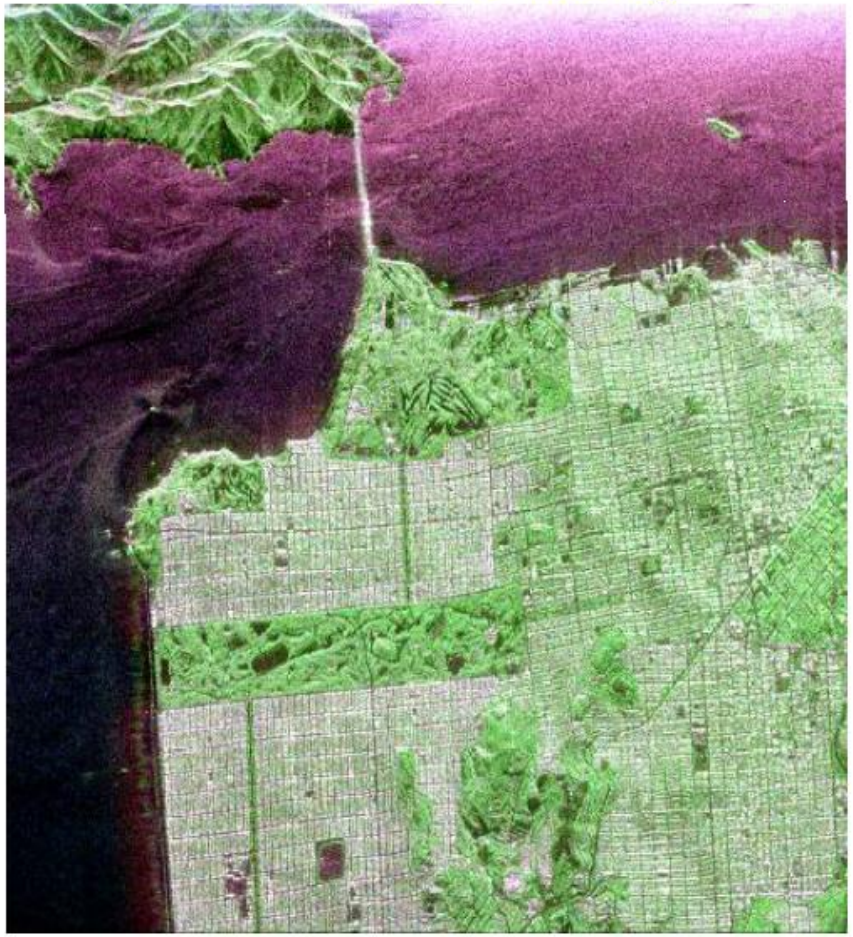

|HH| |HV| |VV|

3) Polarimetric decompositions

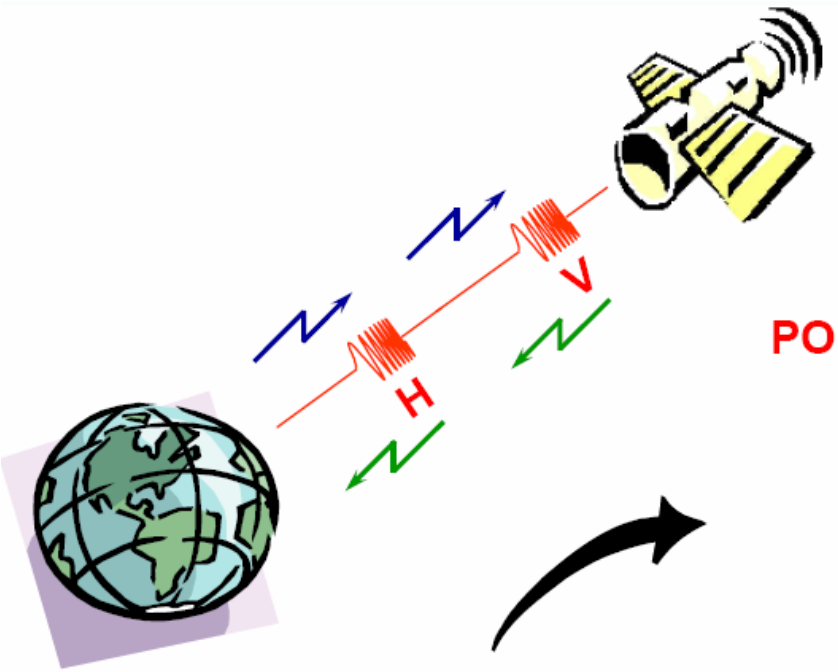

TRANSMITTER: H & V
RECEIVERS: H & V

POLARIMETRIC DESCRIPTORS

[S] SINCLAIR Matrix

$$[S] = \begin{bmatrix} S_{HH} & S_{HV} \\ S_{VH} & S_{VV} \end{bmatrix}$$

$\underline{k}$ Target Vector

[T] 3x3 COHERENCY Matrix

RADAR SCATTERING

PHYSICAL INTERPRETATION

SINGLE BOUNCE SCATTERING
(ROUGH SURFACE)

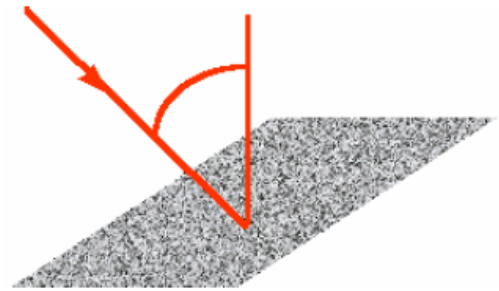

DOUBLE BOUNCE SCATTERING

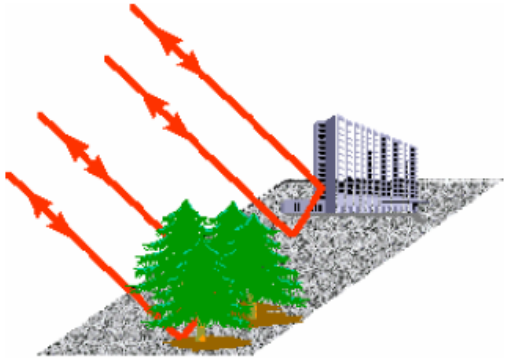

VOLUME SCATTERING

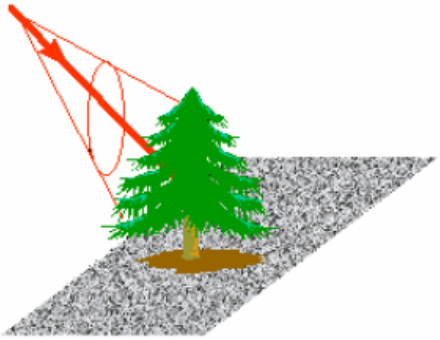

$$T_{11} = 2A_0 = |S_{HH} + S_{VV}|^2$$

$$T_{33} = B_0 - B = 2|S_{HV}|^2$$

$$T_{22} = B_0 + B = |S_{HH} - S_{VV}|^2$$

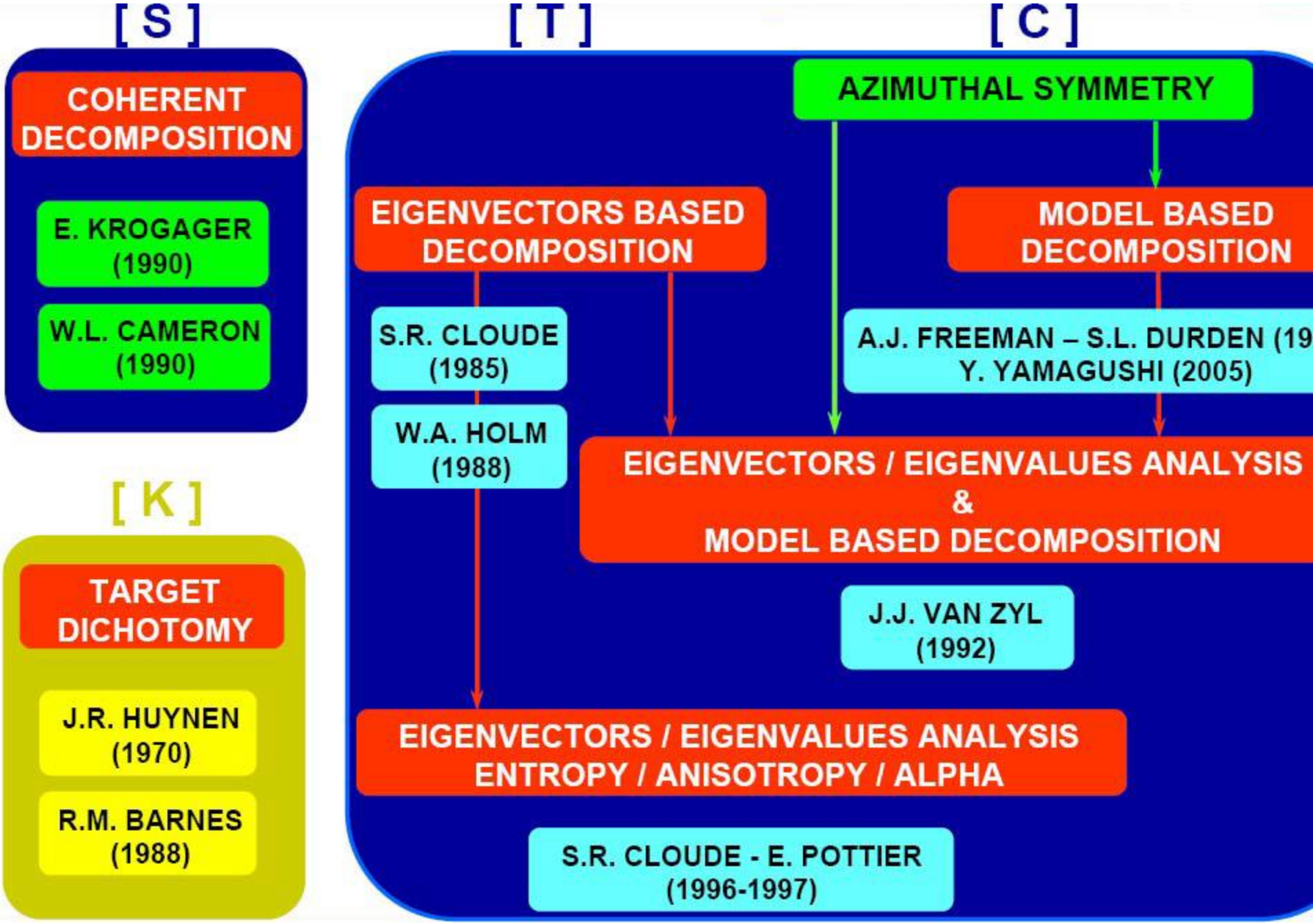
[S]
COHERENT DECOMPOSITION
E. KROGAGER (1990)
W.L. CAMERON (1990)
[K]
TARGET DICHOTOMY
J.R. HUYNEN (1970)
R.M. BARNES (1988)
[T]
[C]
AZIMUTHAL SYMMETRY
EIGENVECTORS BASED DECOMPOSITION
MODEL BASED DECOMPOSITION
S.R. CLOUDE (1985)
W.A. HOLM (1988)
A.J. FREEMAN – S.L. DURDEN (19
Y. YAMAGUSHI (2005)
EIGENVECTORS / EIGENVALUES ANALYSIS & MODEL BASED DECOMPOSITION
J.J. VAN ZYL (1992)
EIGENVECTORS / EIGENVALUES ANALYSIS ENTROPY / ANISOTROPY / ALPHA
S.R. CLOUDE - E. POTTIER (1996-1997)

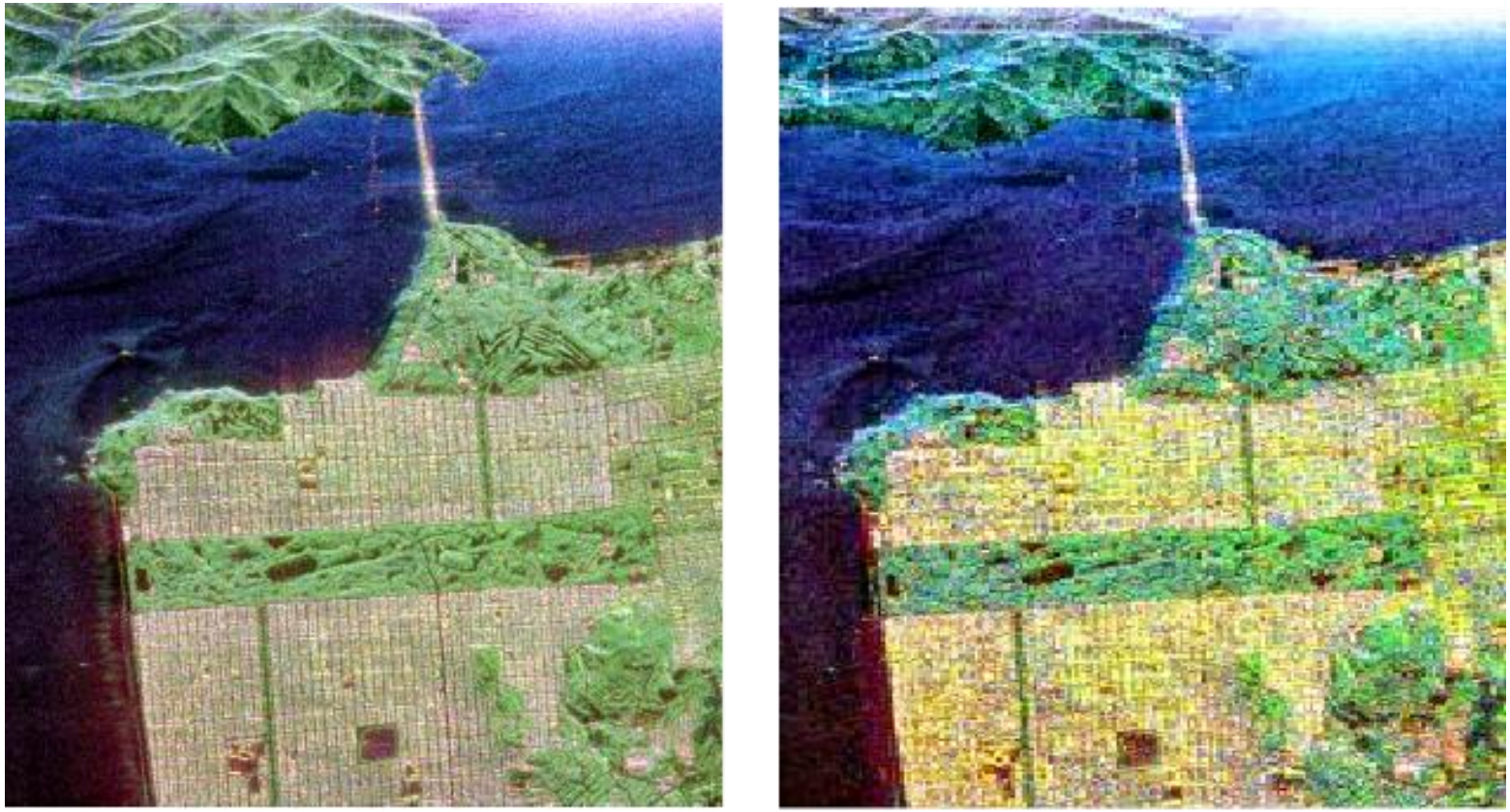

|HH+VV| |HV | |HH-VV|

Comparison of Polarimetric color-coded images in the Pauli basis of the of San Francisco Bay: a) original image,
b) reconstructed image from the dominant scattering mechanism,

Some methods based on orthogonal scattering mechanisms

$$\boldsymbol{T} = \boldsymbol{U}\boldsymbol{\Lambda}\boldsymbol{U}^H = \sum_{i=1}^{3} \lambda_i \boldsymbol{u}_i \boldsymbol{u}_i^H \qquad \lambda_i \geq \lambda_{i+1} \qquad \boldsymbol{u}_j^H \boldsymbol{u}_i = \delta_{i-j}$$

Mechanism of dominant or medium scattering

A first approach, proposed by Cloude [CLO 86b], consists in considering only the dominant mechanism, in other words, whose associated intensity is the highest.

$$\mathbf{S}_{rel} \equiv \sqrt{\lambda_1}\, \boldsymbol{v}_1 = \mathbf{k}_1$$

$$\mathbf{k}_1 = \frac{1}{\sqrt{2}} \begin{bmatrix} S_{hh} + S_{vv} \\ S_{hh} - S_{vv} \\ 2S_{hv} \end{bmatrix} = \begin{bmatrix} \sqrt{2A_0} \\ \sqrt{B_0 + B}\, e^{j\arg(C+jD)} \\ \sqrt{B_0 - B}\, e^{j\arg(G+jH)} \end{bmatrix} = \boldsymbol{k}_1^H \mathbf{k}_1 \begin{bmatrix} \cos\alpha \\ \sin\alpha \cos\beta\, e^{j\delta} \\ \sin\alpha \sin\beta\, e^{j\gamma} \end{bmatrix}$$

The mecanism is qualified as a simple reflexion if $A_0 \gg B_0 + B \text{ et } B_0 - B$

The mecanism is qualified as a double reflexion if $B_0 + B \gg A_0 \text{ et } B_0 - B$

Otherwise scattering by anisotropic particle

H/A/α Decomposition (Cloude 95, Cloude 96)

$$T = U\Lambda U^H = span\sum_{i=1}^{3} p_i u_i u_i^H = span\sum_{i=1}^{3} p_i T_i$$

$$u_i = \begin{bmatrix} \cos\alpha_i \\ \sin\alpha_i \cos\beta_i e^{j\delta_i} \\ \sin\alpha_i \cos\beta_i e^{j\gamma_i} \end{bmatrix}$$

$$\langle [T] \rangle = [U_3][\Sigma][U_3]^{-1} = [u1 \quad u2 \quad u3] \begin{bmatrix} \lambda_1 & 0 & 0 \\ 0 & \lambda_2 & 0 \\ 0 & 0 & \lambda_3 \end{bmatrix} [u1 \quad u2 \quad u3]^{*T}$$

Orthogonal eigenvectors $\lambda_1 > \lambda_2 > \lambda_3$ $P_i = \dfrac{\lambda_i}{\sum_{k=1}^{3} \lambda_k}$

eigenvalues

Entropy: $H = -\sum_{i=1}^{3} P_i \log_3(P_i)$ → has low values over environments with low complexity

Parameter α: $\overline{\alpha} = P_1\alpha_1 + P_2\alpha_2 + P_3\alpha_3$ →qualify the type of wave-matter interaction

Anisotropy: $A = \dfrac{\lambda_2 - \lambda_3}{\lambda_2 + \lambda_3}$ → Complementary to H for areas with two dominant mechanisms

H/A/a decomposition

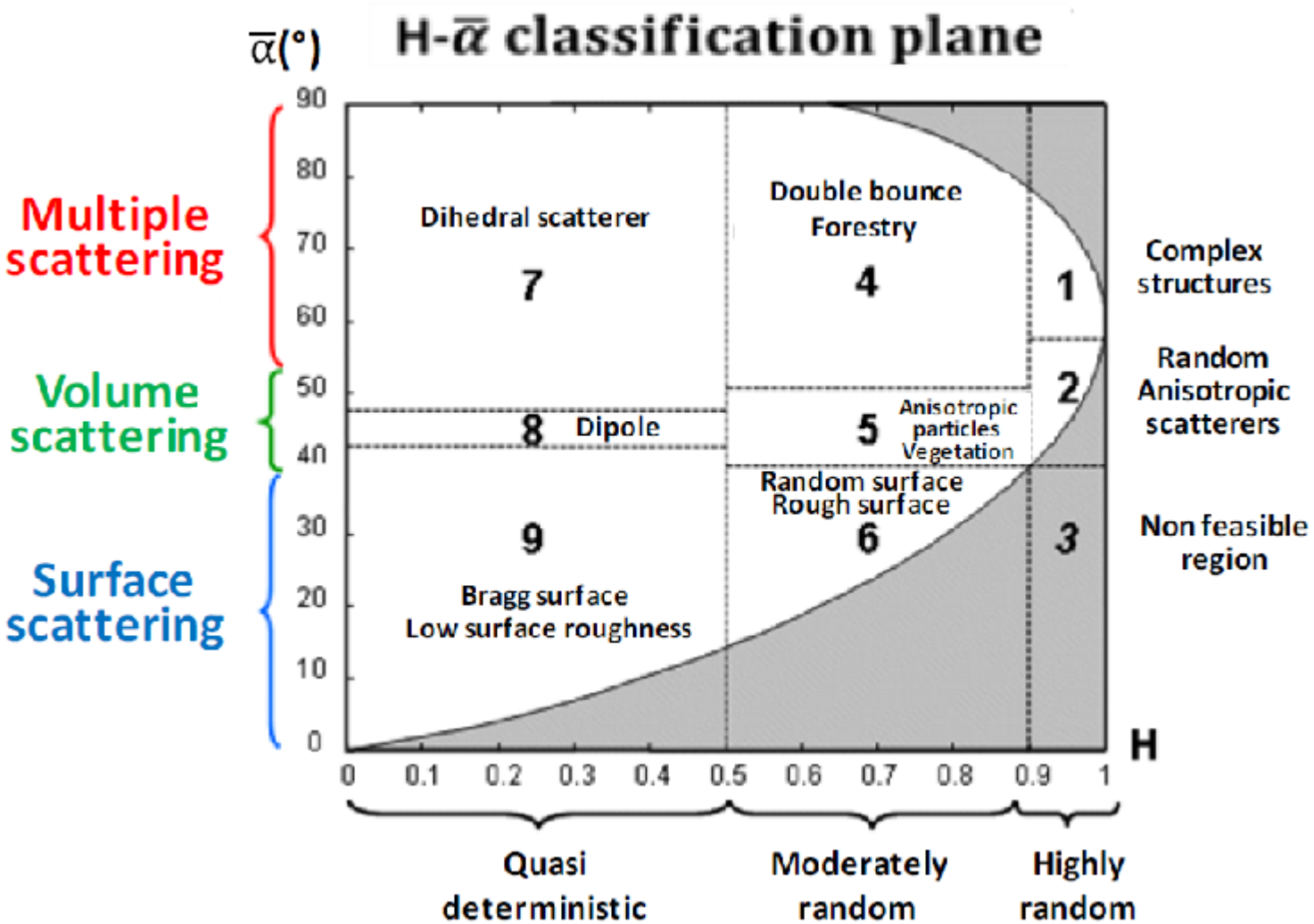

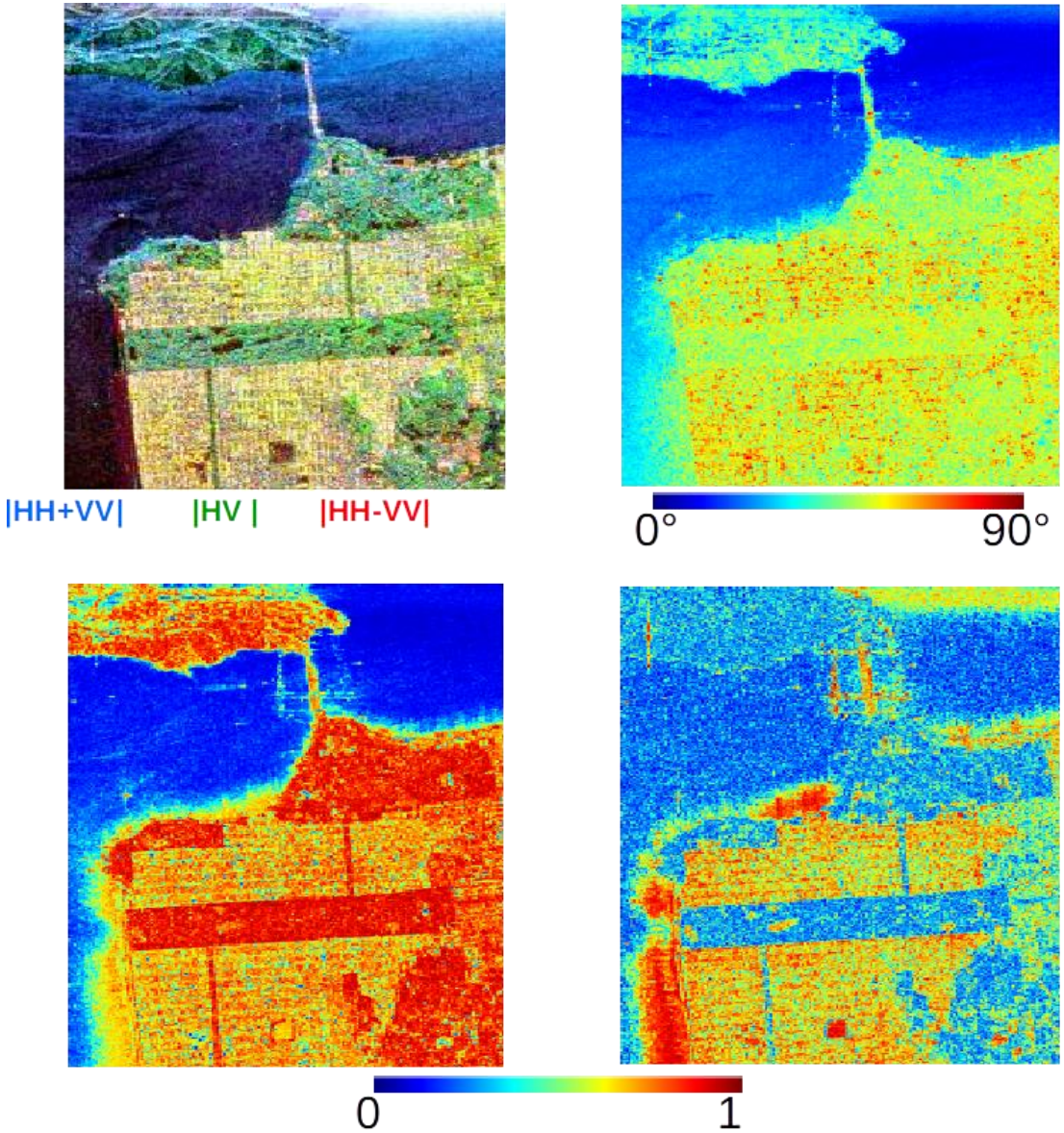

Results of the eigen-decomposition at the San Francisco Bay: a) Pauli image, b) α c) H, d) A

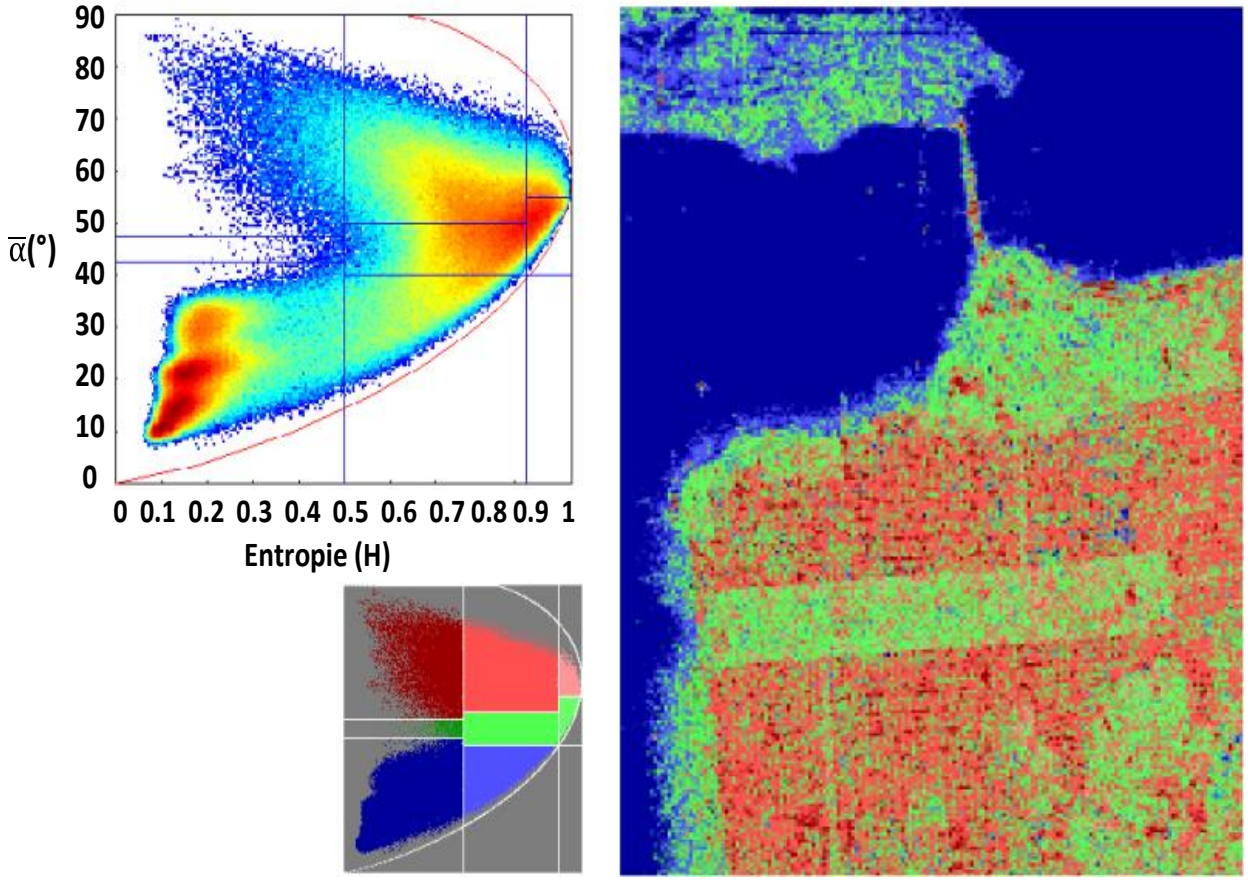

Classification $H - \bar{\alpha}$ of the San Francisco bay image: a) density of the image pixel projection in the $(H, \bar{\alpha})$ domain and color coding, b) classified image

Interferometry

- Complexe SAR image,
- Two informations (amplitude, phase)
- Phase: sum of two contributions

$$\phi = \phi_{geom} + \phi_{propre}$$

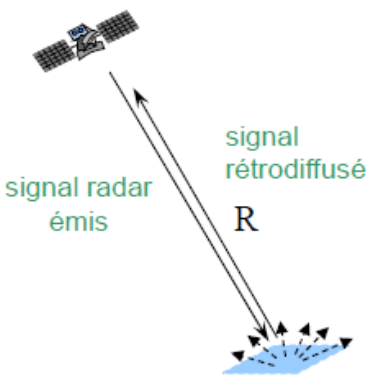

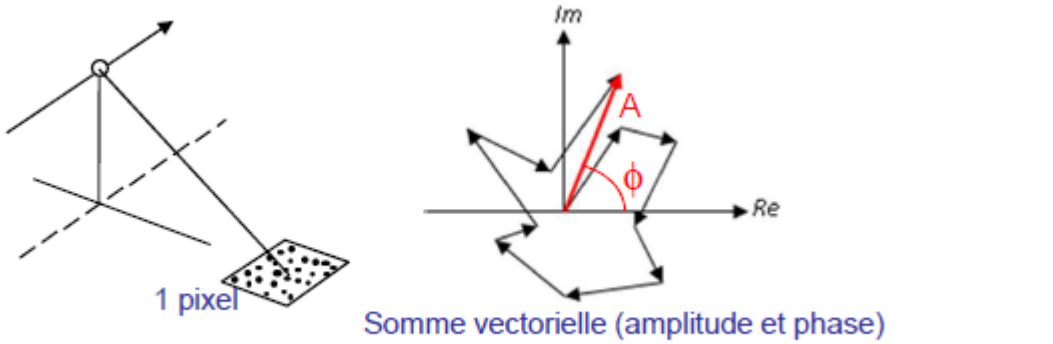

Pixel phase signature (internal contribution)
Vectorial addition of reflectors (amplitude, phase)

$$\phi_{geom} = {}^{4\pi R}/_{\lambda}$$

R: distance between radar and pixel

Coherency

$$\gamma = \frac{\left| \sum_n z_1 z_2^* \right|}{\sqrt{\sum_n |z_1|^2 \sum_n |z_2|^2}}$$

Measurement of phase stability between two images

$$0 \leq \gamma \leq 1$$

Loss of coherency

•Geometric (the satellite does not observe the same points), important change in satellite angle configuration

•Temporal (surface modification between two acquisitions)

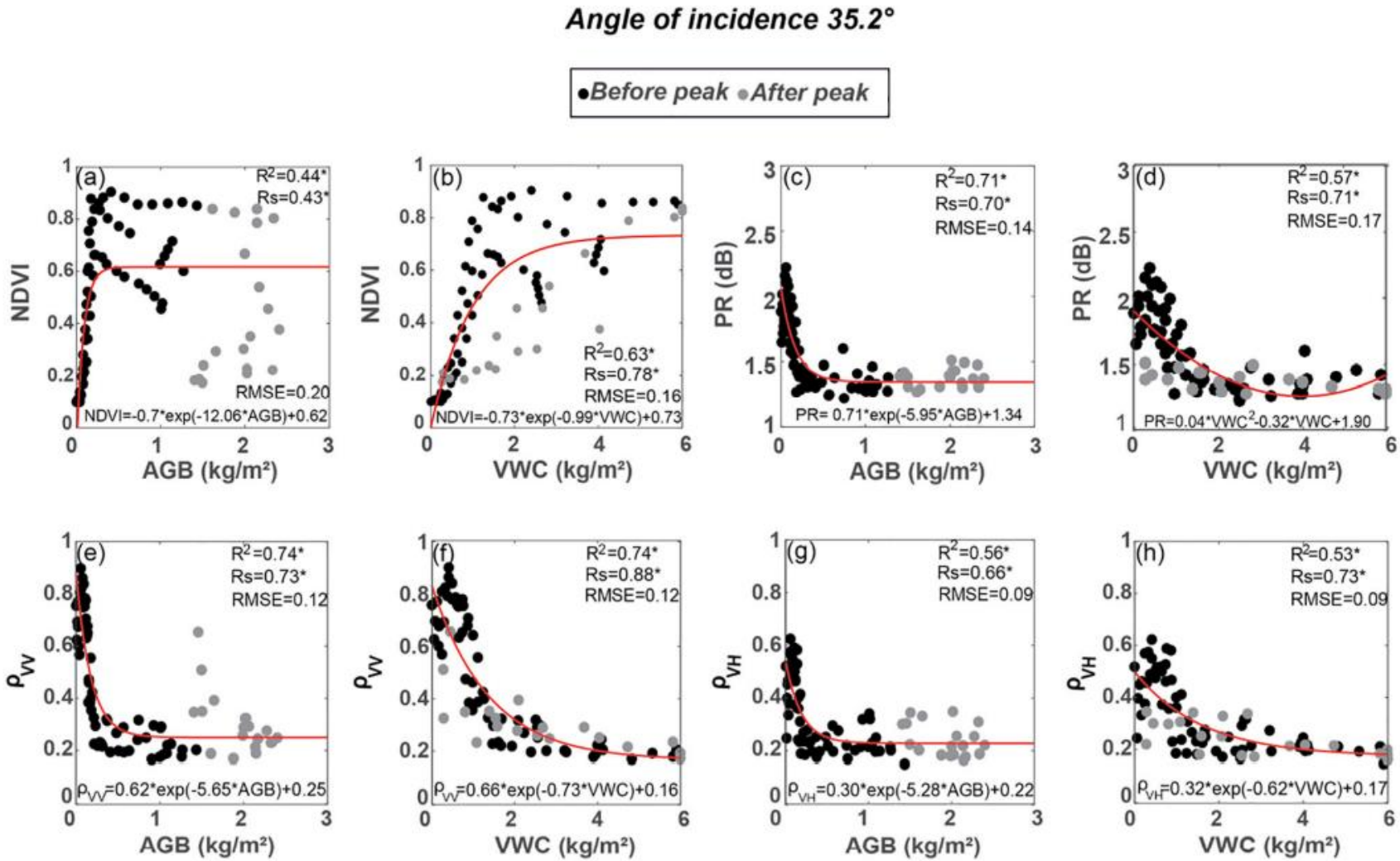

Fig. 5. Relationship between (a, b) NDVI and AGB and VWC; (c, d) PR and AGB and VWC; (e, f) ρ_{VV} and AGB and VWC; (g, h) ρ_{VH} and AGB and VWC at 35.2°. Black point corresponds to data acquired before the AGB (or VWC) peak while grey is for data after the peak. R^2 and Rs significant at the 99% are followed by a star (*).